buffer, fractionated by 10% SDS–PAGE and transferred onto membranes. The membranes were incubated with primary antibodies against HIF-1α (Santa Cruz Biotechnology, Santa Cruz, CA, USA), Akt and phospho-Akt (Cell Signaling Technology, Beverly, MA, USA), and α-tubulin (Lab Vision, Fremont, CA, USA), and then reacted with an HRP-conjugated secondary antibody (BD Transduction Laboratories, San Diego, CA, USA). Positive signals were detected with an enhanced chemiluminescence system (Amersham, Piscataway, NJ, USA). In each study, the experiments were performed in duplicate and repeated 3–5 times ($n = 3$–5). Representative data are shown.

2.3. MTT activity assay

To evaluate the effects of hypoxia and ACh on the mitochondrial function of cardiomyocytes, we measured 3-(4,5-dimethylthiazol-2-yl)-2,5-diphenyl tetrazolium bromide (MTT) reduction activity in H9c2 or HEK293 cells under hypoxia (1% oxygen concentration), in the presence or absence of ACh. The cells were pretreated with 1 mM ACh for 12 h, and then subjected to hypoxia for 12 h. At 4 h before sampling, the MTT reagents were added to the culture and incubated.

2.4. Caspase-3 activity assay

Caspase-3 activity was measured using a CPP32/Caspase-3 Fluorometric Protease Assay Kit, (Chemicon International, Temecula, CA, USA). Hypoxia-treated H9c2 cells with or without 1 mM ACh pretreatment were lysed and the cytosolic extract was added to the caspase-3 substrate. A fluorometer equipped with a 400-nm excitation filter and 505-nm emission filter was used to measure the samples.

2.5. DePsipher assay

To examine the effects of hypoxia and ACh on the mitochondrial electrochemical gradient, we analyzed cardiomyocytes using a DePsipher™ Mitochondrial Potential Assay Kit (Trevigen, Gaithersburg, Maryland, USA). Apoptotic cells, which undergo mitochondrial membrane potential collapse cannot accumulate the DePsipher reagent in their mitochondria. As a result, apoptotic cells show decreased red fluorescence in their mitochondria, and the reagent remains in the cytoplasm as a green fluorescent monomer. Therefore, apoptotic cells were easily differentiated from healthy cells, which showed more red fluorescence.

2.6. Evaluation of NO production

NO production was measured using the 4,5-diaminofluoresceindiacetate (DAF-2DA; Alexis, Lausen, Switzerland) fluorometric NO detection system as previously reported [10]. The intensity of the DAF-2DA green fluorescence in ACh-treated cells was measured and compared with that in non-treated cells (λ_{Ex} 492 nm; λ_{Em} 515 nm).

2.7. Transfection

To investigate the direct contribution of Akt phosphorylation to HIF-1α stabilization or that of HIF-1α to the ACh effect, HEK293 cells were transfected with an expression vector for wild-type Akt (wt Akt), dominant-negative Akt (dn Akt) [11], wild-type HIF-1α (wt HIF-1α) [12] or dominant-negative HIF-1α (dn HIF-1α), using Effectene (Qiagen, Valencia, CA, USA) according to the manufacture's protocol. After transfection, HEK293 cells were pretreated with 1 mM ACh for 12 h, followed by evaluating the HIF-1α protein level or by hypoxia for 12 h and MTT activity in each group was evaluated. As a control, cells were transfected with a vector for green fluorescent protein (GFP).

2.8. RT-PCR

Total RNA was isolated from H9c2 cells according to a modified acid guanidinium–phenol–chloroform method using an RNA isolation kit (ISOGEN; Nippon Gene, Tokyo, Japan), and reverse-transcribed to obtain a first-strand cDNA. This first-strand cDNA was amplified by specific primers for HIF-1α, and the PCR products were fractionated by electrophoresis.

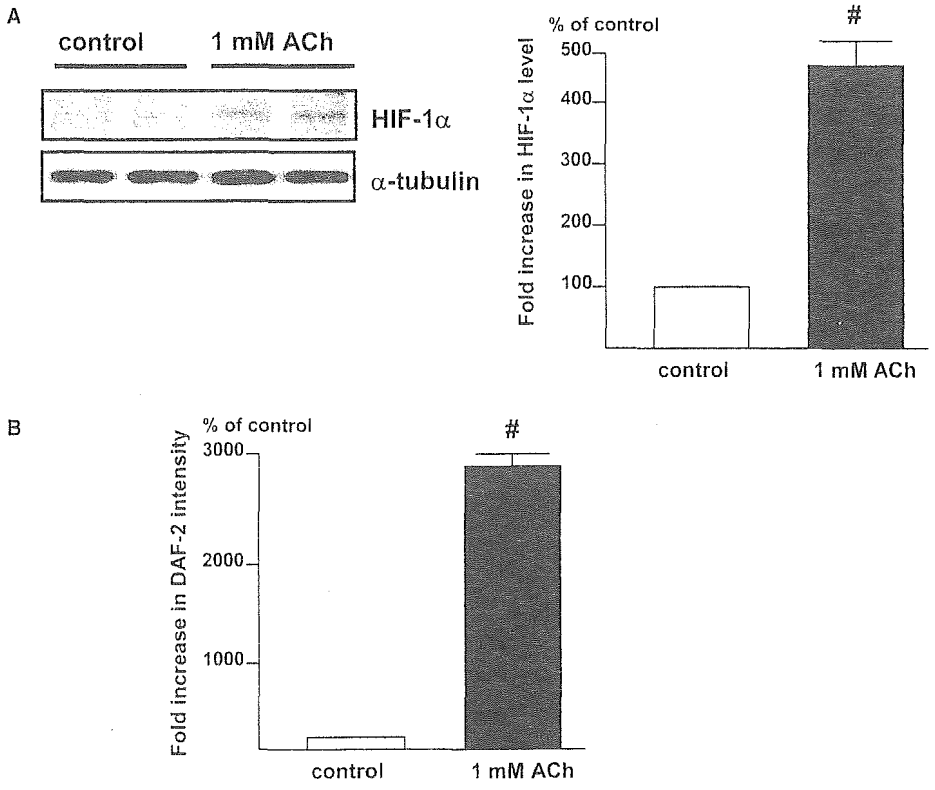

Fig. 1. HIF-1α is induced by ACh in rat cardiomyocytes even under normoxia. (A) After treatment of H9c2 cells with 1 mM ACh for 8 h, the HIF-1α protein level is increased ($^{\#}P < 0.05$ vs. control, $n = 4$). (B) ACh (1 mM) increases the intensity of DAF-2DA fluorescence ($^{\#}P < 0.01$ vs. control, $n = 3$).

2.9. Vagal nerve stimulation in myocardial ischemia

Left ventricular myocardial ischemia (MI) was performed by 3 h of left coronary artery (LCA) ligation in anesthetized 9-week-old male Wistar rats under artificial ventilation previously described [2]. Sham-operated (control) rats did not undergo LCA ligation. For vagal nerve stimulation (VS), the right vagal nerve in the neck was isolated and cut. Only the distal end of the vagal nerve was stimulated in order to exclude the effects of the vagal afferent. The electrode was connected to an isolated constant voltage stimulator. VS was performed from 1 min before the LCA ligation until 3 h afterwards, using 0.1 ms pulses at 10 Hz (MI-VS). The electrical voltage of the pulses was adjusted to obtain a 10% reduction in the heart rate before LCA ligation, but VS (MI-VS) was not associated with any blood pressure reduction during the experiments, compared with MI. At the end of the experiments, the rats were either injected with 2 ml of 2% Evans blue dye via the femoral vein to measure the risk area followed by determination of the infarct size with 2% triphenyl tetrazolium chloride (TTC) staining or the heart was excised for protein isolation and subsequent Western Blotting to detect HIF-1α protein. The percentage of the infarcted area of the left ventricle was calculated as the ratio of the infarcted area to the risk area.

2.10. Densitometry

The Western Blotting data were analyzed using Kodak 1D Image Analysis Software (Eastman Kodak Co., Rochester, NY, USA).

2.11. Statistics

The data were presented as means ± S.E. The mean values between two groups were compared by the unpaired Student's *t* test. Differences among data were assessed by ANOVA for multiple comparisons of results. Differences were considered significant at $P < 0.05$.

3. Results

3.1. Posttranslational regulation of HIF-1α by ACh through a non-hypoxic pathway

ACh (1 mM) increased HIF-1α protein expression in H9c2 cells under normoxia (Fig. 1A). ACh increased NO production, as evaluated by DAF-2DA (Fig. 1B), suggesting that

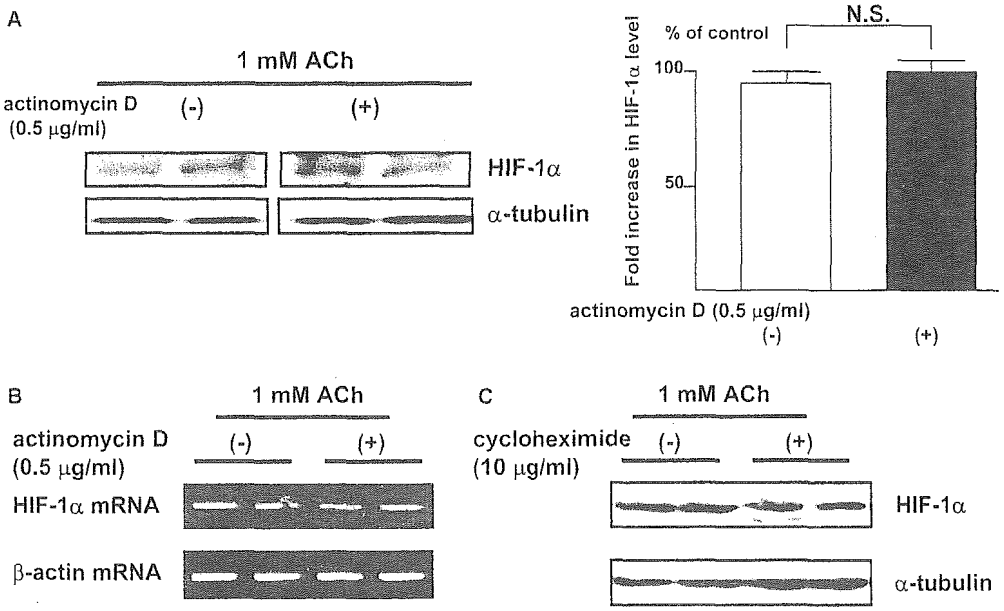

Fig. 2. HIF-1α induction by ACh is posttranslationally regulated in rat cardiomyocytes under normoxia. (A) The HIF-1α protein level in H9c2 cells in the presence of 0.5 μg/ml of actinomycin D is increased by 1 mM ACh to a comparable level to that in the absence of actinomycin D (N.S., not significant, $n = 3$). (B) Actinomycin D does not decrease the HIF-1α mRNA level, as evaluated by RT-PCR. (C) Cycloheximide (10 μg/ml) does not affect the HIF-1α protein level ($n = 3$).

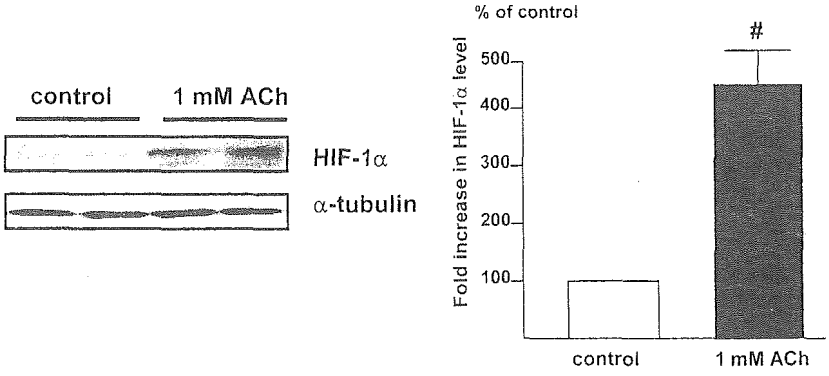

Fig. 3. Rat primary cultured cardiomyocytes show comparable HIF-1α induction by 1 mM ACh to that in H9c2 cells ($^{\#}P < 0.05$ vs. control, $n = 3$).

NO is involved in the signal transduction of HIF-1α induction. Actinomycin D (0.5 μg/ml; Figs. 2A and B) and cycloheximide (10 μg/ml; Fig. 2C) did not decrease the HIF-1α level under normoxia, suggesting that HIF-1α degradation is regulated by ACh. Furthermore, ACh increased HIF-1 α level in primary cardiomyocytes without reducing their beating rate (Fig. 3). Since H9c2 cells did not beat, these results suggest that HIF-1 induction is independent of the heart rate-decreasing effect of ACh.

3.2. Akt phosphorylation by ACh

ACh had no effect on the total Akt protein level, but increased Akt phosphorylation (Fig. 4A) as effectively as SNAP (data not shown). The ACh-induced Akt phosphorylation was inhibited by atropine in a dose-dependent manner (Fig. 4B). ACh-induced Akt phosphorylation and its inhibition by atropine were also observed in rat primary cardiomyocytes (Fig. 4C).

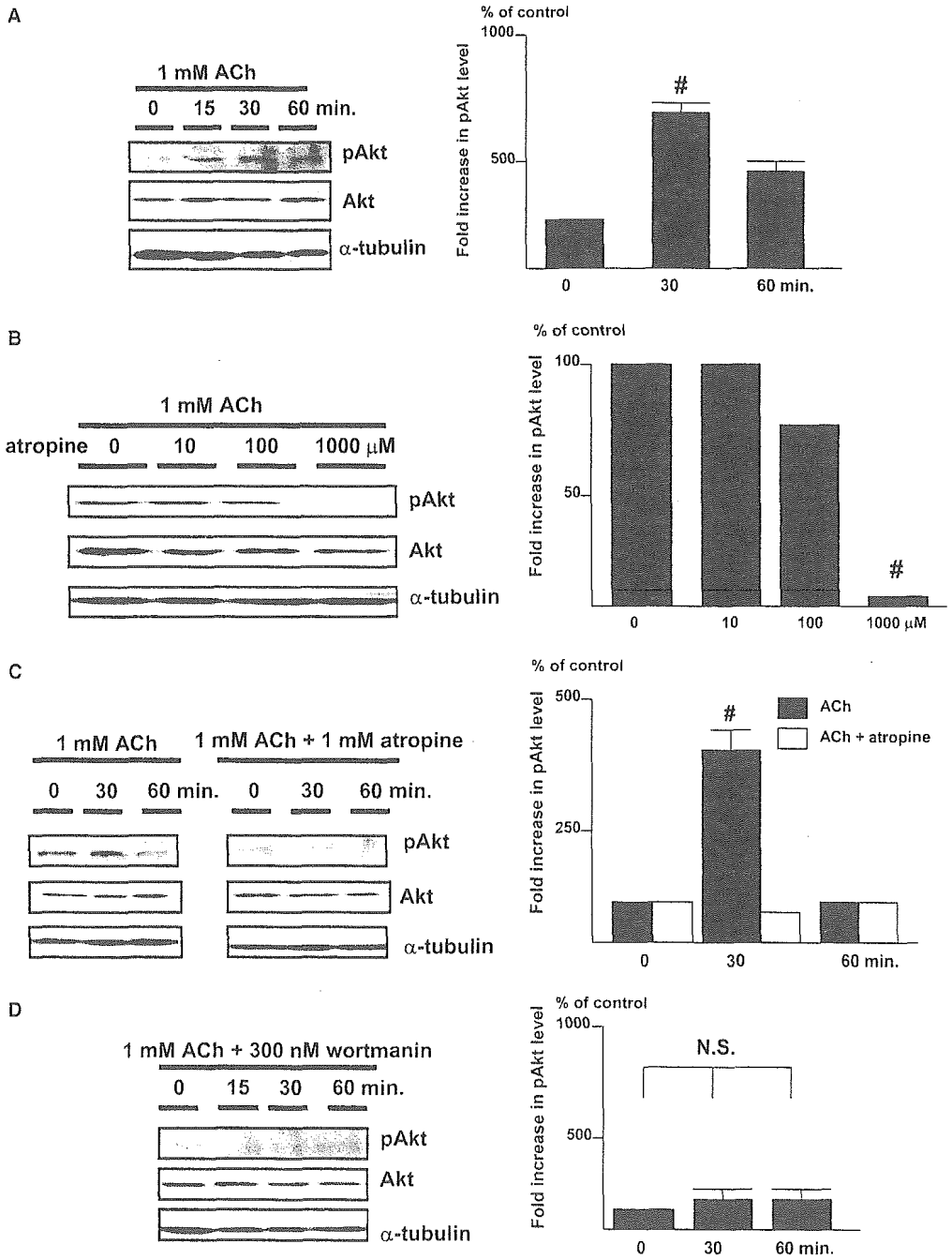

Fig. 4. Akt is activated by ACh in rat cardiomyocytes, leading to HIF-1α induction. (A) Akt phosphorylation in H9c2 cells is rapidly increased by 1 mM ACh ($^{\#}P < 0.05$ vs. baseline, $n = 4$), whereas the total protein level of Akt remains unaffected. (B) The ACh-induced increase in Akt phosphorylation is blocked by 1 mM atropine ($^{\#}P < 0.05$ vs. 0 μM atropine, $n = 3$). (C) ACh (1 mM) also increases Akt phosphorylation in rat primary cardiomyocytes ($^{\#}P < 0.05$ vs. baseline, $n = 3$), and atropine blocks this effect. (D) Pretreatment with 300 nM wortmannin completely inhibits ACh-induced Akt phosphorylation in H9c2 cells (N.S., not significant, $n = 3$). (E) Wortmannin (300 nM) also inhibits HIF-1α induction by ACh ($^{\#}P < 0.05$ vs. wortmannin (+), $n = 3$). Each figure shows a representative result from three independently performed experiments ($n = 3$). (F) In contrast to wt Akt, HIF-1α induction by ACh is blocked by dn Akt in HEK293 cells ($n = 4$).

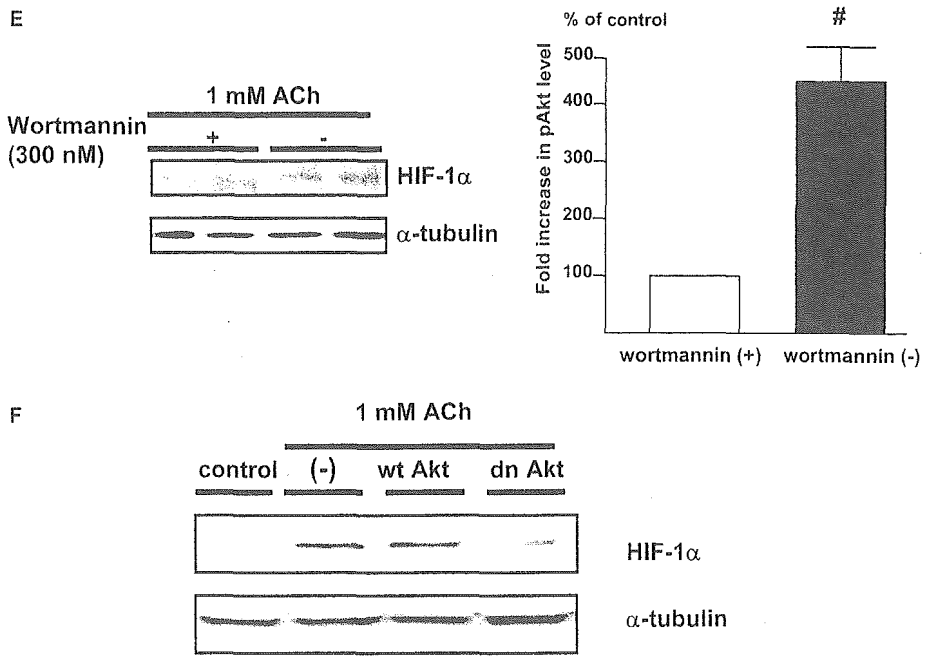

Fig. 4 (*continued*)

3.3. PI3K/Akt Pathway for HIF-1α induction by ACh

Wortmannin completely inhibited the ACh-induced Akt phosphorylation (Fig. 4D), in clear contrast to the data in Fig. 4A. Furthermore, it also attenuated the HIF-1α induction by ACh (Fig. 4E). To elucidate the contribution of Akt phosphorylation to HIF-1α protein level in normoxia, dn Akt was introduced into HEK293 cells, and found to partially inhibit the HIF-1α induction by ACh (Fig. 4F).

3.4. Effect of ACh on apoptosis during hypoxia

The DePsipher assay clearly showed that hypoxia (1% oxygen concentration) for 12 h caused mitochondrial membrane potential collapse leading to cell death, and that 1 mM ACh inhibited this collapse in H9c2 cells (Fig. 5A). ACh attenuated the decrease in MTT activity caused by 12 h of hypoxia in H9c2 cells (Fig. 5B; 103.4 ± 0.8% in ACh + hypoxia vs. 56.6 ± 0.7% in hypoxia, $P < 0.01$, $n = 8$) and HEK293 cells ($P < 0.01$ vs. hypoxia). The caspase-3 activity was increased by hypoxia in H9c2 cells, and pretreatment with 1 mM ACh inhibited this increase (Fig. 5C; 128 ± 2% in hypoxia vs. 90 ± 2% in ACh + hypoxia, $P < 0.01$, $n = 4$). To elucidate the dependency of the ACh-induced protective effect on HIF-1α, dn HIF-1α was transfected into HEK293 cells, followed by ACh pretreatment and then hypoxia. It was found that dn HIF-1α inhibited the protective effect of ACh from hypoxia (Fig. 5D; 115.1 ± 1.2% in wt HIF-1α and 111.8 ± 1.8% in GFP vs. 59.0 ± 3.4% in dn HIF-1α, $P < 0.05$, $n = 10$), suggesting that HIF-1α induction by ACh is partially responsible for the protective effect.

3.5. Effect of vagal stimulation on HIF-1α in myocardial ischemia

To evaluate the significance of ACh for cardioprotection in vivo, the vagal nerve was stimulated prior to the MI. Histological analysis demonstrated a tendency for the infarcted area from the vagal nerve-stimulated (MI-VS) hearts to be smaller than that from non-stimulated (MI) hearts (31.5 ± 4.6% in MI-VS vs. 40.9 ± 2.5% in MI, $n = 3$), even though the risk areas (non-perfused areas) were comparable (Fig. 6A; 59.2 ± 1.0% in MI-VS vs. 53.7 ± 1.0% in MI, $n = 3$). In the MI-VS hearts, the HIF-1α protein level was further elevated compared to that in the MI hearts (Fig. 6B; 244 ± 24% in MI-VS vs. 112 ± 1% in MI, $n = 3$). These results suggest that vagal nerve stimulation in the ischemic heart activates both the hypoxic and non-hypoxic pathways of HIF-1α induction, resulting in increased induction of HIF-1α.

3.6. Non-hypoxic induction of HIF-1α in other cells

The observed ACh-mediated HIF-1 induction was not limited to H9c2 or primary cultured cardiomyocytes, but also found in several other types of cell lines, including HEK293, and HeLa cells (Fig. 7). Since these cells did not beat spontaneously, the results suggest that the system of ACh-mediated HIF-1α induction is not only independent of the beating rate of cardiomyocytes, but also a generally conserved system in cells.

4. Discussion

4.1. Cardioprotective action by ACh and vagal stimulation via the muscarinic receptor

Using animal models, several studies have shown that accentuated antagonism against the sympathetic nervous system is a major mechanism for the beneficial effect of vagal tone on the ischemic heart [13]. Although ACh was involved in triggering preconditioning mechanisms in an ischemia-reperfusion model [3], it remained unclear whether vagal nerve stimulation in acute ischemia or hypoxia followed these mechanisms. In the present study, we have disclosed that ACh possesses a

protective effect on cardiomyocytes. In rat cardiomyocytes, ACh triggered a sequence of survival signals through Akt that eventually induced HIF-1α, inhibited the collapse of the mitochondrial membrane potential and decreased caspase-3 activity, thereby leading to the survival of cardiomyocytes under hypoxia. Furthermore, our results suggest ACh exerts this action through Akt in other cells. The current study therefore provides another insight into the cellular mechanism for the cardioprotective effects of ACh and vagal stimulation.

4.2. *Signaling pathway of ACh via PI3K/Akt and antiapoptotic effects of ACh*

Since previous studies demonstrated that a PI3K inhibitor greatly reduced HIF-1α induction in heart and renal cells [14,15] and a few studies have reported that MAP kinase is activated through ACh, we focused on the PI3K/Akt pathway, one of the important cell survival signaling pathways [16], and found that ACh directly activated Akt phosphorylation via PI3K. PI3K/Akt signaling has been reported to have an

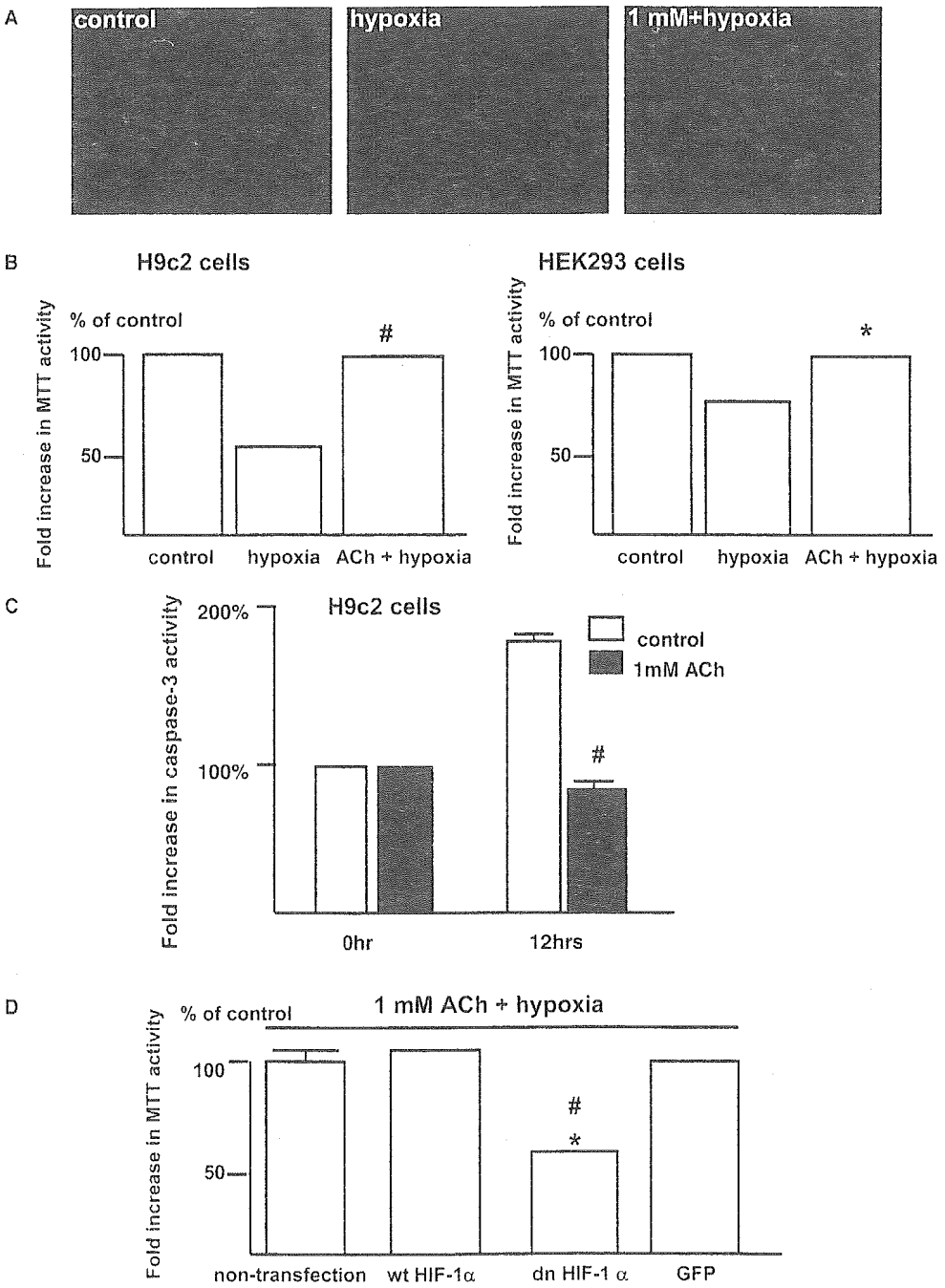

Fig. 5. Collapse of the mitochondrial membrane potential in rat cardiomyocytes under hypoxia is attenuated by ACh pretreatment. (A) Hypoxia decreases the mitochondrial membrane potential in H9c2 cells within 12 h. Red spots are decreased by hypoxia, whereas pretreatment with 1 mM ACh for 12 h inhibits this effect. (B) Pretreatment with 1 mM ACh inhibits the decrease in MTT reduction activity induced by 12 h of hypoxia not only in H9c2 cells ($^{\#}P < 0.01$ vs. hypoxia, $n = 8$) but also in HEK293 cells ($^{*}P < 0.01$ vs. hypoxia, $n = 8$). (C) Hypoxia increases caspase-3 activity, whereas pretreatment with 1 mM ACh inhibits this effect ($^{\#}P < 0.01$ vs. hypoxia, $n = 3$). (D) In contrast to wt HIF-1α or GFP, dn HIF-1α alone decreases the MTT activity under hypoxia after ACh treatment ($^{\#}P < 0.01$ vs. wt and GFP, $^{*}P < 0.05$ vs. non-transfection, $n = 10$).

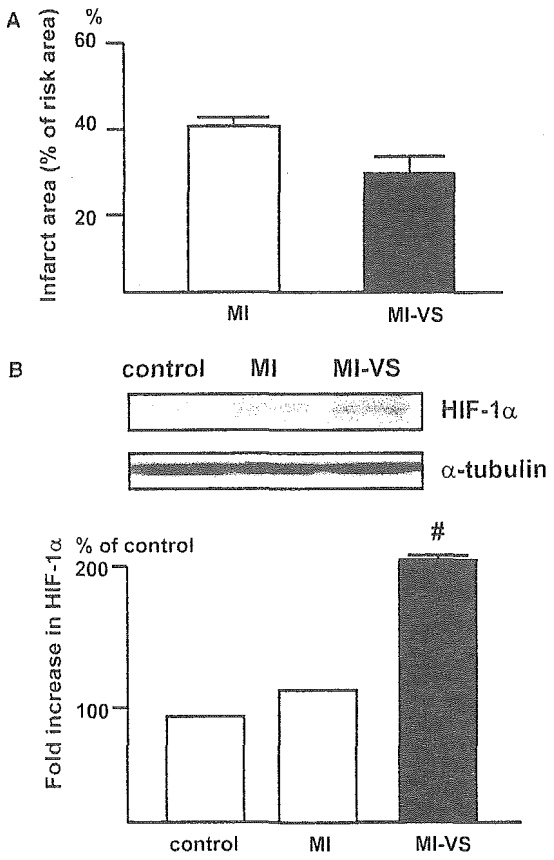

Fig. 6. Vagal nerve stimulation decreases infarcted area with increased HIF-1α expression. (A) A quantitative analysis reveals comparable non-perfused areas in both vagal-stimulated (MI-VS) and non-stimulated (MI) hearts, whereas the infarcted area identified by TTC staining is smaller in the MI-VS heart than in the MI heart. (B) HIF-1α induction in the ischemic heart is increased by vagal stimulation (MI-VS) compared with that in ischemia alone (MI) ($^{\#}P < 0.01$ vs. MI) ($n = 3$).

antiapoptotic activity through various features, such as inhibition of Bad-binding to Bcl-2, caspase 9, Fas and glycogen synthetase kinase-3 [17,18]. These facts imply a definite involvement of Akt activation in cell survival. As shown using dn HIF-1α, ACh inhibited hypoxia-induced cell death through HIF-1α induction via Akt phosphorylation. These results indicate that ACh actually protects cardiomyocytes from hypoxia at the cellular level.

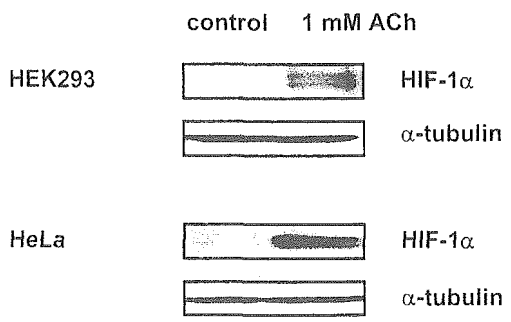

Fig. 7. HIF-1α is induced by ACh under normoxia in other cells. ACh (1 mM) increases HIF-1α protein level in HEK293 and HeLa cells ($n = 3$ each) under normoxia.

4.3. Additional induction of HIF-1α by ACh and vagal stimulation

HIF-1α regulates the transcriptional activities of very diverse genes involved in cell survival and is itself regulated at the posttranslational level by VHL [4,6,7]. Recent studies have shown that HIF-1α is also regulated through a non-hypoxic pathway involving angiotensin II, TNF-α and NO [8,9,19,20]. Therefore, it is speculated that cardiomyocytes possess a similar system for regulating HIF-1α through ACh, independent of the oxygen concentration. Induction of HIF-1α is a powerful cellular response against hypoxia, and further increases in its expression by other pathways may be beneficial. The present results indicate that the significance of ACh or vagal nerve stimulation in hypoxic stress can be attributed to additional HIF-1α induction through dual induction pathways, i.e., hypoxic and non-hypoxic pathways.

The present study has revealed that ACh-mediated HIF-1α induction is widely conserved in other cells. Consistent with a previous report [10], the current results suggest that NO is produced by ACh. According to a report that NO attenuates the interaction between pVHL and HIF-1α through inhibiting PHD activity [21], it is possible that ACh may increase the HIF-1α protein level through NO. Recent studies conducted by Krieg et al. [3] and Xi et al. [22], have provided supportive data compatible with our results, while another study by Hirota et al. [23] also revealed a non-hypoxic pathway for HIF-1α induction by ACh in a human kidney-derived cell line.

The signaling pathway of the muscarinic receptor has been studied extensively, and many pathways are involved in its specific biological effects. Therefore, possible involvement of other pathways in the non-hypoxic induction of HIF-1α cannot be excluded. However, it was demonstrated that dn Akt and dn HIF-1α decreased the effect of ACh. Consistent with a recent study [24], we have revealed that ACh or vagal stimulation protects cardiomyocytes in the acute phase. This observation suggests that the protective effect in the acute phase may result in inhibition of cardiac remodeling in the chronic phase, since vagal stimulation produces additional HIF-1α induction through a non-hypoxic pathway, which increases cell survival.

Acknowledgment: This study was supported by a Health and Labor Sciences Research Grant (H15-PHYSI-001) for Advanced Medical Technology from the Ministry of Health, Labor, and Welfare of Japan.

References

[1] Julian, D.G., Camm, A.J., Frangin, G., Janse, M.J., Munoz, A., Schwartz, P.J. and Simon, P. (1997) Randomised trial of effect of amiodarone on mortality in patients with left-ventricular dysfunction after recent myocardial infarction: EMIAT. European Myocardial Infarct Amiodarone Trial Investigators. Lancet 349, 667–674.

[2] Li, M., Zheng, C., Sato, T., Kawada, T., Sugimachi, M. and Sunagawa, K. (2004) Vagal nerve stimulation markedly improves long-term survival after chronic heart failure in rats. Circulation 109, 120–124.

[3] Krieg, T., Qin, Q., Philipp, S., Alexeyev, M.F., Cohen, M.V. and Downey, J.M. (2004) Acetylcholine and bradykinin trigger preconditioning in the heart through pathway that includes Akt and NOS. Am. J. Physiol. Heart Circ. Physiol. 287, H2606–H2611.

[4] Semenza, G.L. (2003) HIF-1, O(2), and the 3 PHDs: how animal cells signal hypoxia to the nucleus. Cell 107, 1–3.
[5] Kakinuma, Y., Miyauchi, T., Yuki, K., Murakoshi, N., Goto, K. and Yamaguchi, I. (2001) Novel molecular mechanism of increased myocardial endothelin-1 expression in the failing heart involving the transcriptional factor hypoxia-inducible factor-1α induced for impaired myocardial energy metabolism. Circulation 103, 2387–2394.
[6] Maxwell, P.H., Wiesener, M.S., Chang, G.W., Clifford, S.C., Vaux, E.C., Cockman, M.E., Wykoff, C.C., Pugh, C.W., Maher, E.R. and Ratcliffe, P.J. (1999) The tumour suppressor protein VHL targets hypoxia-inducible factors for oxygen-dependent proteolysis. Nature 399, 271–275.
[7] Min, J.H., Yang, H., Ivan, M., Gertler, F., Kaelin Jr, W.G. and Pavletich, N.P. (2002) Structure of an HIF-1alpha-pVHL complex: hydroxyproline recognition in signaling. Science 296, 1886–1889.
[8] Page, E.L., Robitaille, G.A., Pouyssegur, J. and Richard, D.E. (2002) Induction of hypoxia-inducible factor-1alpha by transcriptional and translational mechanisms. J. Biol. Chem. 277, 48403–48409.
[9] Richard, D.E., Berra, E. and Pouyssegur, J. (2000) Non-hypoxic pathway mediates the induction of hypoxia-inducible factor 1alpha in vascular smooth muscle cells. J. Biol. Chem. 275, 26765–26771.
[10] Zanella, B., Calonghi, N., Pagnotta, E., Masotti, L. and Guarnieri, C. (2002) Mitochondrial nitric oxide localization in H9c2 cells revealed by confocal microscopy. Biochem. Biophys. Res. Commun. 290, 1010–1014.
[11] Okudela, K., Hayashi, H., Ito, T., Yazawa, T., Suzuki, T., Nakane, Y., Sato, H., Ishi, H., KeQin, X., Masuda, A., Takahashi, T. and Kitamura, H. (2004) K-ras gene mutation enhances motility of immortalized airway cells and lung adenocarcinoma cells via Akt activation: possible contribution to non-invasive expansion of lung adenocarcinoma. Am. J. Pathol. 164, 91–100.
[12] Chen, J., Zhao, S., Nakada, K., Kuge, Y., Tamaki, N., Okada, F., Wang, J., Shindo, M., Higashino, F., Takeda, K., Asaka, M., Katoh, H., Sugiyama, T., Hosokawa, M. and Kobayashi, M. (2004) Dominant-negative hypoxia-inducible factor-1 alpha reduces tumorigenicity of pancreatic cancer cells through the suppression of glucose metabolism. Am. J. Pathol. 162, 1283–1291.
[13] Du, X.J., Dart, A.M., Riemersma, R.A. and Oliver, M.F. (1990) Failure of the cholinergic modulation of norepinephrine release during acute myocardial ischemia in the rat. Circ. Res. 66, 950–956.
[14] Kim, C.H., Cho, Y.S., Chun, Y.S., Park, J.W. and Kim, M.S. (2002) Early expression of myocardial HIF-1alpha in response to mechanical stresses: regulation by stretch-activated channels and the phosphatidylinositol 3-kinase signaling pathway. Circ. Res. 90, e25–e33.
[15] Sandau, K.B., Zhou, J., Kietzmann, T. and Brune, B. (2001) Regulation of the hypoxia-inducible factor 1alpha by the inflammatory mediators nitric oxide and tumor necrosis factor-alpha in contrast to desferroxamine and phenylarsine oxide. J. Biol. Chem. 276, 39805–39811.
[16] Vanhaesebroeck, B. and Alessi, D.R. (1999) The regulation and activities of the multifunctional serine/threonine kinase Akt/PKB. Exp. Cell Res. 253, 210–229.
[17] Kennedy, S.G., Wagner, A.J., Conzen, S.D., Jordan, J., Bellacosa, A., Tsichlis, P.N. and Hay, N. (1997) The PI3-kinase/Akt signaling pathway delivers an anti-apoptotic signal. Genes Dev. 11, 701–713.
[18] Cross, D.A., Alessi, D.R., Cohen, P., Andjelkovich, M., Hemmings, B.A. and Inhibition of glycogen synthase kinase-3 by insulin mediated by protein kinase, B. (1995) Nature 378, 785–789.
[19] Zhou, J., Schmid, T. and Brune, B. (2003) Tumor necrosis factor-alpha causes accumulation of a ubiquitinated form of hypoxia inducible factor-1alpha through a nuclear factor-kappaB-dependent pathway. Mol. Biol. Cell 14, 2216–2225.
[20] Sandau, K.B., Fandrey, J. and Brune, B. (2001) Accumulation of HIF-1alpha under the influence of nitric oxide. Blood 97, 1009–1015.
[21] Metzen, E., Zhou, J., Jelkmann, W., Fandrey, J. and Brune, B. (2003) Nitric oxide impairs normoxic degradation of HIF-1alpha by inhibition of prolyl hydroxylases. Mol. Biol. Cell 14, 3470–3481.
[22] Xi, L., Taher, M., Yin, C., Salloum, F. and Kukreja, R.C. (2004) Cobalt chloride induces delayed cardiac preconditioning in mice through selective activation of HIF-1{alpha}/AP-1 and iNOS signaling. Am. J. Physiol. Heart. Circ. Physiol. 287, H2369–H2375.
[23] Hirota, K., Fukuda, R., Takabuchi, S., Kizaka-Kondoh, S., Adachi, T., Fukuda, K. and Semenza, G.L. (2004) Induction of hypoxia-inducible factor 1 activity by muscarinic acetylcholine receptor signaling. J. Biol. Chem. 279, 41521–41528.
[24] Wang, H., Yu, M., Ochani, M., Amella, C.A., Tanovic, M., Susarla, S., Li, J.H., Wang, H., Yang, H., Ulloa, L., Al-Abed, Y., Czura, C.J. and Tracey, K.J. (2003) Nicotinic acetylcholine receptor alpha7 subunit is an essential regulator of inflammation. Nature 421, 384–388.

Original Paper

nephron
Experimental
Nephrology

Nephron Exp Nephrol 2005;100:e95–e103
DOI: 10.1159/000084575

Received: August 31, 2004
Accepted: December 8, 2004
Published online: March 17, 2005

Hypoxia-Inducible Factor-1α Is Involved in the Attenuation of Experimentally Induced Rat Glomerulonephritis

Yoshihiro Kudo[a] Yoshihiko Kakinuma[b] Yasukiyo Mori[e]
Norihito Morimoto[a] Takashi Karashima[c] Mutsuo Furihata[d]
Takayuki Sato[b] Taro Shuin[c] Tetsuro Sugiura[a]

Departments of [a]Laboratory Medicine, [b]Cardiovascular Control, [c]Urology and [d]Tumor Pathology, Kochi Medical School, Kochi, and [e]The Second Department of Internal Medicine, Kansai Medical University, Osaka, Japan

Key Words
Glomerulonephritis · Habu snake venom · Angiotensin II · Hypoxia-inducible factor-1α

Abstract

Background/Aim: Among various kidney disease models, there are few rat glomerulonephritis (GN) models that develop in a short time, and with mainly glomerular lesions. Hypoxia-inducible factor (HIF)-1α is a transcriptional factor that induces genes supporting cell survival, but the involvement of HIF-1α in attenuating the progression of GN remains to be elucidated. We developed a new model of rat GN by coadministration of angiotensin II (AII) with Habu snake venom (HV) and investigated whether HIF-1α is involved in renal protection. ***Methods:*** Male Wistar rats were unilaterally nephrectomized on day 1, and divided into 4 groups on day 0; N group (no treatment), HV group, A group (AII), and H+A group (HV and AII). To preinduce HIF-1α, cobalt chloride ($CoCl_2$) was injected twice before injections of HV and AII in 11 rats. ***Results:*** GN was detected only in the H+A group; observed first on day 2 and aggravated thereafter. HIF-1α was expressed in the glomeruli and renal tubules in the A and H+A groups. In the H+A group, GN was remarkably reduced by $CoCl_2$ pretreatment (44.9 to 12.2%, $p < 0.01$). ***Conclusion:*** Both HV and AII were critical for the development of GN, and HIF-1α remarkably attenuated the progression of GN.

Introduction

Many animal studies have been performed in attempts to overcome the poor prognosis of chronic renal failure due to diabetic nephropathy and glomerulonephritis (GN) [1–5]. Although factors involved in the pathogenesis of GN have been intensively investigated, the development of a proper animal GN model with high reproducibility and simplicity as well as a model without time-consuming process is required. Experimental rat models of GN are classified into several groups in terms of the pathophysiological mechanisms of renal diseases. Anti-glomerular basement membrane nephritis was developed with depositions of immune complex using anti-glomerular basement membrane antibody [3, 6], tubulointerstitial injury was caused by cyclosporine A [4] and injury of renal tubules by ischemia [5]. However, there are few rat GN models with mainly pathological features in the glo-

KARGER
Fax + 41 61 306 12 34
E-Mail karger@karger.ch
www.karger.com

1660–2129/05/1002–0095$22.00/0

Accessible online at:
www.karger.com/nee

Yoshihiko Kakinuma, MD, PhD
Department of Cardiovascular Control
Kochi Medical School
Nankoku, Kochi 783-8505 (Japan)
Tel. +81 88 880 2311, Fax +81 88 880 2310, E-Mail kakinuma@med.kochi-u.ac.jp

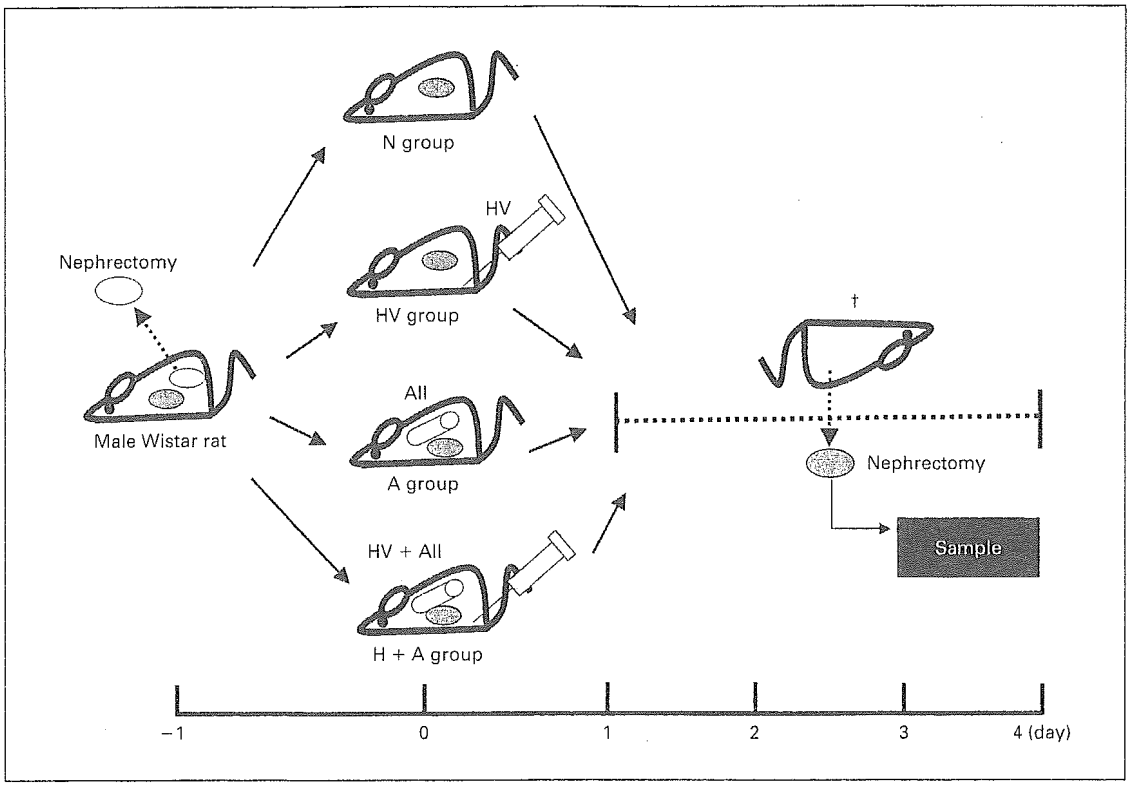

Fig. 1. Study Protocol. All rats are unilaterally nephrectomized on day 1 and divided into 4 groups on day 0. N group: no injection of reagents. HV group: injection of 3.5 mg/kg of Habu snake venom (HV). A group: continuous administration of 100 ng/min of angiotensin II (AII). H+A group: administration of HV and AII.

meruli that are developed in a short time [7]. Angiotensin II (AII) is known to increase blood pressure through vascular contraction, and to be profoundly involved in cardiovascular hypertrophy and the contraction of intrarenal arteries. AII is also directly involved in the progression of glomerulosclerosis via the effect of hyperfiltration with or without hypertension [8, 9]. Many studies have revealed important factors involved in the pathogenesis of GN or factors aggravating GN, but evaluating further factors that suppress the occurrence of GN is also crucial. To investigate the features of renal protection, we focused on hypoxia-inducible factor (HIF)-1α. HIF-1α, a transcriptional factor with formation of a heterodimer with HIF-1β [10], is post-transcriptionally regulated and its protein level is elevated by hypoxia through inhibition of ubiquitin-mediated degradation. HIF-1α is known to be a survival factor responsible for inducing lines of genes supporting cell survival such as glucose metabolism (glucose transporters and glycolytic enzymes), vasomotor regulation (heme oxygenase-1 and endothelin-1), angiogenic growth (vascular endothelial growth factor), and anemia control (erythropoietin and transferrin) [11–13]. Recent studies have demonstrated that non-hypoxic stimuli like AII can also activate HIF-1α [14, 15], but the role of HIF-1α induction in attenuating the progression of GN remains to be elucidated. Accordingly, we developed a new rat GN model by coadministration of AII with Habu snake venom (HV) and investigated whether preinduction of HIF-1α leads to renal protection.

Materials and Methods

Development of Rat GN Model

All experiments were approved by the institutional review board for the care of animal subjects and were performed in accordance with guidelines of Kochi Medical School. Nine-week-old male Wistar rats (180–220 g) were purchased from Japan SLC (Shizuoka, Japan). Rats were unilaterally nephrectomized on day 1. On day 0, the rats were divided into 4 groups. In the first group, no treatment was performed with any reagents or surgical procedure (N group, n = 6). In the second group, rats were injected with 3.5 mg/kg of HV (Sigma-Aldrich Co., Steinheim, Germany) through the femoral vein (HV group, n = 11). In the third group, rats were continuously adminis-

tered with AII (100 ng/min; Peptide Institute Inc., Osaka, Japan) using Alzet osmotic pumps (DURECT Co., Cupertino, Calif., USA) (A group, n = 11). In the fourth group, rats were administered with both HV and AII (H+A group, n = 22). Rats were sacrificed on day 1, 2, 3 or 4, and kidneys excised for histochemical analysis (fig. 1).

Measurement of Systolic Blood Pressure

Systolic blood pressure (SBP) was measured by the tail-cuff method with an electro-sphygmomanometer (BP-98A; Softron Co., Tokyo, Japan). SBP was measured in conscious rats every day from day 1 to 2. The SBP value for each rat was calculated as the average of 3 separate measurements at each session. SBP measurement was performed between 9 and 12 a.m. by a single blinded investigator.

Measurements of Serum Urea Nitrogen and Creatinine

Before the sacrifice, blood samples were obtained via an axillary vein for determination of serum urea nitrogen (UN) and creatinine (Cr) levels. Serum UN and Cr levels were determined enzymatically with automation-analysis equipment (Hitachi 7350; Hitachi Co., Ibaragi, Japan) in our laboratory center.

Histological Analysis

To evaluate the progression of GN in our animal model, histological analyses were performed using the periodic acid-Schiff (PAS) and periodic acid-methenamine silver (PAM) reagents. After the specimens were paraffin embedded, 4-μm-sectioned samples were stained with PAS and PAM reagents and counterstained with hematoxylin. For quantitative analysis, the ratio of damaged glomeruli to all glomeruli in the sectioned sample was calculated and the percentage of GN in the section was evaluated. Moreover, semiquantitative analysis was performed to evaluate more precisely the morphological changes of our GN model according to the protocol in previous studies [16, 17]. A minimum of 20 glomeruli (ranging from 20 to 60 glomeruli) in each specimen were examined and the severity of the mesangiolysis lesion was graded from 0 to 4+ according to the percentage of glomerular involvement; a 1+ lesion represented an involvement of 25% of the glomerulus while a 4+ lesion indicated that 100% of the glomerulus was involved. Thus, the mesangiolysis score (MES) was then obtained by multiplying the degree of damage (0 to 4+) by the percentage of the glomeruli with the lesion. Tubular injuries including tubular necrosis or occlusion of collecting ducts by cast material were graded as mild (1+), moderate (2+), or severe (3+).

Western Blot Analysis

Nuclear protein from whole kidney was prepared using NE-PER Nuclear and Cytoplasmic Extraction Reagents (Pierce Biotechnology Inc., Rockford, Ill., USA). Nuclear protein was electrophoresed using 10% SDS-PAGE gels and transferred to polyvinylidene difluoride membrane (Immobilon-P; Millipore Corp., Bedford, Mass., USA). A monoclonal IgG HIF-1α antibody α67 (Novus Biological, Littleton, Colo., USA) was used; a horseradish peroxidase-conjugated antibody (Promega Co., Madison, Wisc., USA) was used as a secondary antibody. The ECL Western blotting systems (Amersham Bioscience, Uppsala, Sweden) was used for detection.

Immunohistochemical Analysis

Paraffin sections including the samples were dewaxed in xylene and rehydrated in a series of ethanol, and then washed in distilled water before staining procedures. According to the instruction provided by the manufacturer, HIF-1α was identified with rabbit polyclonal anti-HIF-1α antibody H-206 (Santa Cruz Biotechnology, Calif., USA) utilizing the catalyzed signal amplification system (Dako, Hamburg, Germany) based on the streptavidin-biotin-peroxidase reaction. Antigen retrieval was performed for 5 min in a preheated Dako target retrieval solution using a microwave. Incubation procedures were performed in a humidified chamber. Following the incubation, specimens were washed 3 times in TBST buffer. The specificity of staining was confirmed by substitution of the primary antibody for a normal rabbit IgG and additionally by an immunohistochemical reaction without a primary antibody but with the secondary antibody alone.

An Experiment Using Cobalt Chloride as a Pretreatment

Rats were twice subcutaneously administered 30 mg/kg of cobalt chloride ($CoCl_2$) at a 12-hour interval ($CoCl_2$ group) (n = 11), followed by unilateral nephrectomy. Then, the rats were administered with HV and AII. As a comparison, rats were injected with 0.9% NaCl solution instead of $CoCl_2$, followed by the same protocol as the $CoCl_2$ group (n = 11). After $CoCl_2$ administration, however, before injection of HV and AII, a kidney was excised as a sample to examine expression level of HIF-1α ($CoCl_2$ Pre). Likewise, 2 days after administration of HV and AII, a kidney was also excised ($CoCl_2$ Day 2). To compare the expression level of HIF-1α by $CoCl_2$ before GN and the severity of pathology of GN, we investigated whether preinduction of HIF-1α is involved in renal protection.

Statistical Analysis

Data are reported as mean ± SEM. A paired t test was used for paired samples and Student's t test was used to compare the 2 groups. One-way layout analysis of variance or repeated measures of analysis of variance were used to compare multiple groups. If the p value was significant, Scheffé's multiple comparison was performed. A p value <0.05 was considered significant.

Results

AII Combined with HV Developed GN

Morphological studies using PAS and PAM staining revealed that there are no glomerular or tubular injuries in N group (fig. 2a), HV group (fig. 2b), A group (fig. 2c), however, GN was detected only in the H+A group (fig. 2e). Although renal tubular casts were observed, glomerular changes were scarcely observed on day 1 after AII and HV administration (fig. 2d, 3). GN was initially detected on day 2 (fig. 2e, f, 3), followed by further aggravation during the time course (data not shown). Renal tubular injury including tubular necrosis was not remarkable, and extensive cellular infiltration was not found in the interstitial regions (fig. 3). On the other hand, characteristic focal and segmental mesangiolysis, explained as capillary aneurysmal ballooning, was observed with dilatation of glomerulus (fig. 2e, f). The rate of occurrence of GN on day 2 was 44.9 ± 2.6%, and the MES score of the H+A

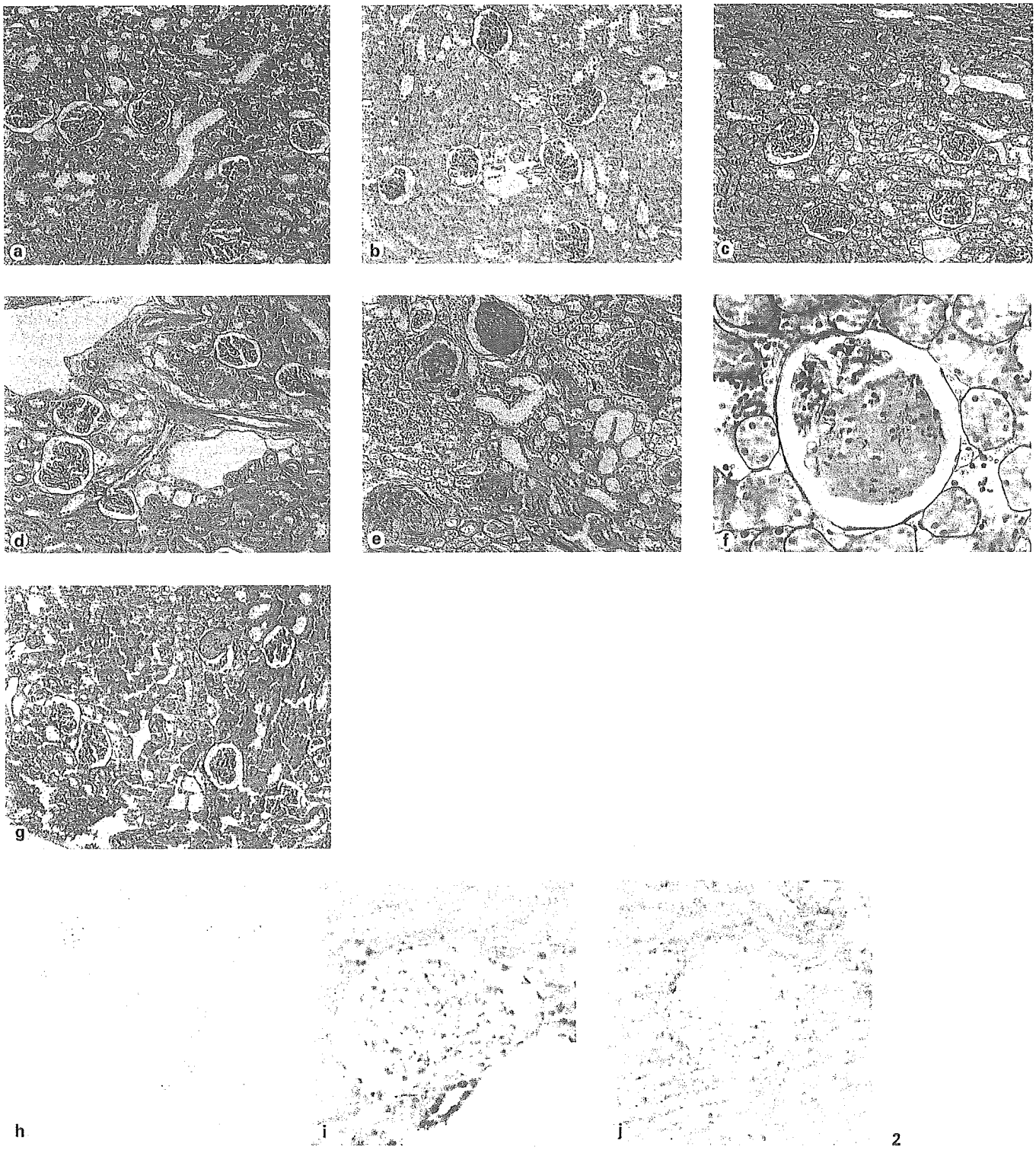

2

group was 199 ± 15 (fig. 3). On the other hand, in the HV group, less than 2% had morphologic changes of mesangiolysis during 4 days, and the MES score was 10 ± 5 (fig. 2b, 3). Moreover, in the A group, there were no morphologic changes during the time course (fig. 2c).

Changes in Serum UN and Cr

Serum UN and Cr were 18.4 ± 0.7 and 0.31 ± 0.01 mg/dl, respectively, on day 2 in the N group. In the H+A group, serum UN and Cr levels increased to 41.5 ± 4.0 and 0.57 ± 0.05 mg/dl, respectively, on day 2; significantly higher than those in the N group (fig. 4a, b). In contrast, serum UN and Cr levels in the H+A group on day 1 (24.0 ± 1.8 and 0.42 ± 0.02 mg/dl, respectively) were similar to the level of the N group. There were no significant differences in serum UN and Cr level among the HV, A and N groups.

SBP Response

SBP values of each group are shown in figure 4c. There were no significant differences in SBP after nephrectomy among the 4 groups. Administration of AII caused a significant increase of SBP on day 1 (186 ± 4 mm Hg) and persisted to day 2 (192 ± 1 mm Hg). SBP in the H+A group on day 2 (183 ± 3 mm Hg) was comparable to that in the A group. Administration of HV had no influence on SBP during the 2 days.

Expression Level of HIF-1α Protein

Western blot analysis revealed that the expression level of HIF-1α protein increased in the H+A and A groups (fig. 5a), compatible with the results of immunohistochemical analysis. Expressions of HIF-1α protein were observed in the A and H+A groups, but protein expression was not detected in the N and HV groups. These data suggest that HIF-1α was induced mainly by AII, and, at least in part, was related to the pathogenesis of GN or to the defense mechanism against the progression of GN.

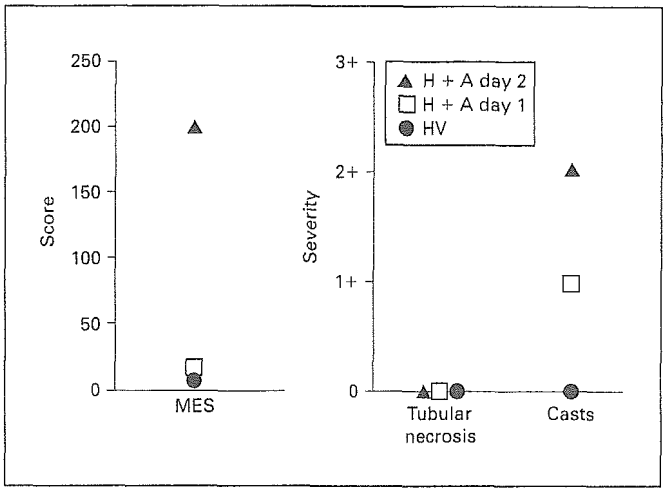

Fig. 3. Semiquantitative analysis of morphologic changes in our glomerulonephritis model. The main lesion in the H+A group is initially detected on day 2 as mesangiolysis in glomeruli; however, there are no tubular lesions of necrosis except for tubular casts; in contrast, there are no morphological changes in the N and A groups. MES = Mesangiolysis score.

Induction of HIF-1α in Glomeruli and Renal Tubules

Immunohistochemical study demonstrated positive nuclear staining of HIF-1α in glomeruli, renal tubules (fig. 2i, j), collecting ducts and epithelium of the papilla (data not shown) in the A and H+A groups. In contrast, no positive nuclear signals were detected in the N (fig. 2h) and HV (data not shown) groups. HIF-1α-positive cells were mainly detected in mesangial cells in glomeruli (fig. 2i, j). As demonstrated, especially in the H+A group (fig. 2j), HIF-1α was expressed in the intact part of the glomerulus, but not in the injured part of the same glomerulus. Furthermore, nuclear HIF-1α-positive signals were observed in smooth muscle cells in peripheral renal arteries (data not shown).

$CoCl_2$ Pretreatment Inhibits the Progression of GN

To further investigate whether HIF-1α is involved in the development of nephropathy or in the antiprogressive action, we pretreated rats with $CoCl_2$. As demonstrated in figure 5b, pretreatment with $CoCl_2$ increased HIF-1α expression before administration of HV and AII (Pre-1),

Fig. 2. Glomerulonephritis is developed with the combination of HV and AII, and HIF-1α is induced in the intact glomeruli. There are no glomerular or tubular injuries in N group (**a**), HV group (**b**), A group (**c**) and H+A group on day 1 (**d**). Damaged glomeruli, characterized by extensive mesangiolysis, are observed in H+A group on day 2. PAS staining. Magnification, ×100 (**e**). Focal and segmental mesangiolysis with large capillary aneurysmal ballooning are observed in the H+A group on day 2. PAM staining. Magnification, ×400 (**f**). The number of GN was significantly less in pretreatment with $CoCl_2$ than without. PAS staining. Magnification, ×100 (**g**). Immunoreactive HIF-1α-positive signals are not detected in the N group (**h**). Nuclear HIF-1α signals are observed in a glomerulus and tubules in the A group. Magnification, ×200 (**i**). A glomerulus in the H+A group on day 2 possesses intact cells with HIF-1α-positive signals; in contrast, other parts have few HIF-1α signals due to mesangiolysis. Magnification, ×200 (**j**).

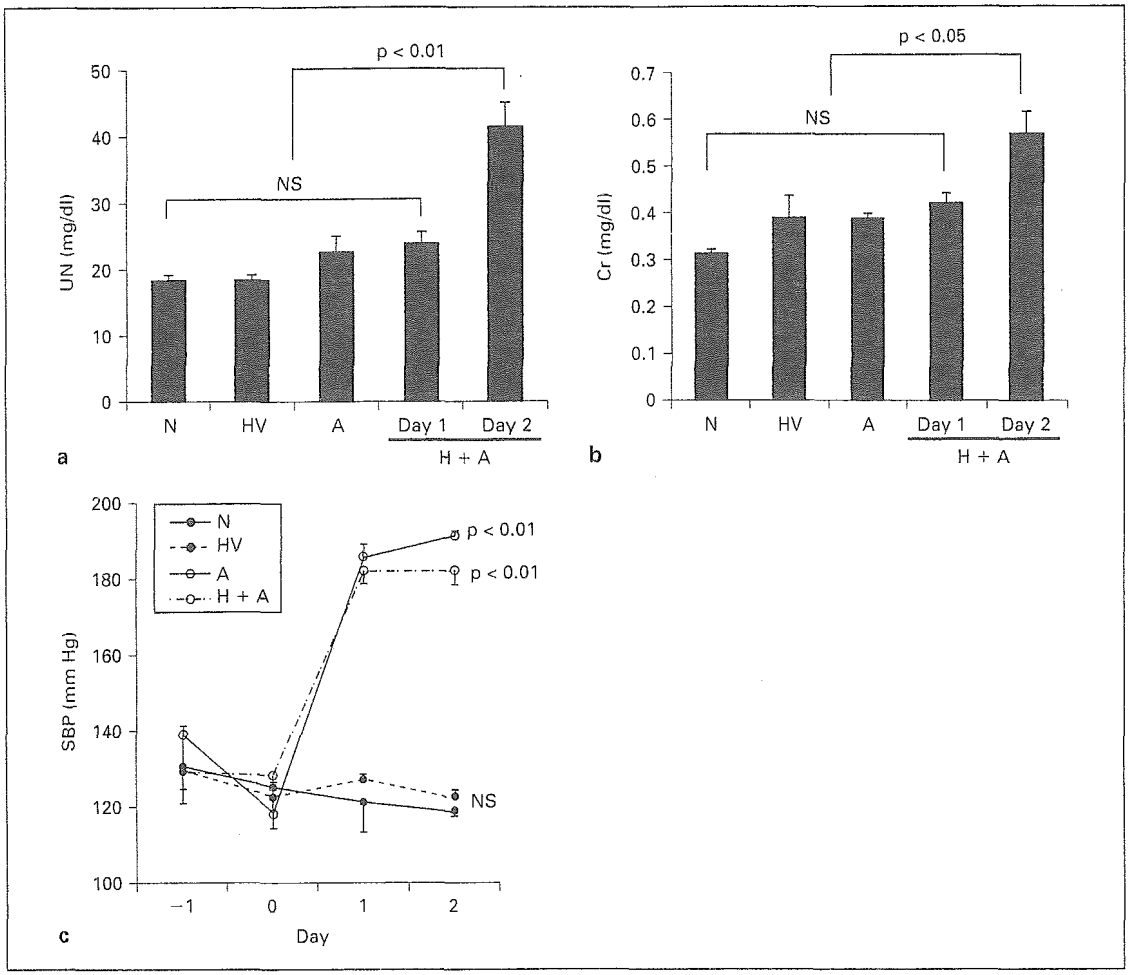

Fig. 4. Serum UN, Cr and SBP are increased with the combination of HV and AII. The serum UN (**a**) and Cr (**b**) levels in the H+A group on day 2 are significantly higher than other groups. SBP increases significantly with administration of AII (A and H+A groups) (**c**).

suggesting that HIF-1α was induced by $CoCl_2$ before development of GN. Even on day 2, the expression level of HIF-1α was increased in the $CoCl_2$ group ($CoCl_2$ Day 2-1). In the $CoCl_2$ group, focal mesangiolysis with glomeruli enlargement was still observed, but the number of GN was much less than in those without $CoCl_2$ pretreatment (fig. 2g).

Thus, 7 of 11 rats (63.6%) with $CoCl_2$ pretreatment were rescued from GN alone, while the other 4 (36.4%) were not; showing a comparable severity level of GN with the non-$CoCl_2$ group. As demonstrated in figure 5b, unlike Pre-1, Pre-2 did not induce HIF-1α with $CoCl_2$ and showed no $CoCl_2$ suppression of GN. The ratio between rats rescued or not rescued from GN was comparable with that between preinduction and noninduction of HIF-1α by $CoCl_2$, as demonstrated in figure 5c. In the $CoCl_2$ group, the rate of GN from each rat decreased to 12.2 ± 2.1%, which was in great contrast to 44.9 ± 2.6% in the non-$CoCl_2$ group. Furthermore, serum UN and Cr levels on day 2 were significantly lower in the $CoCl_2$ than in the non-$CoCl_2$ group ($p < 0.05$) (fig. 6a, b), despite comparable SBP values between the 2 groups (fig. 6c).

Discussion

In this study, we developed a new model of GN induced by both HV and AII. This model has several distinct characteristics. First, GN developed rapidly, and was detected on the second day after administration of

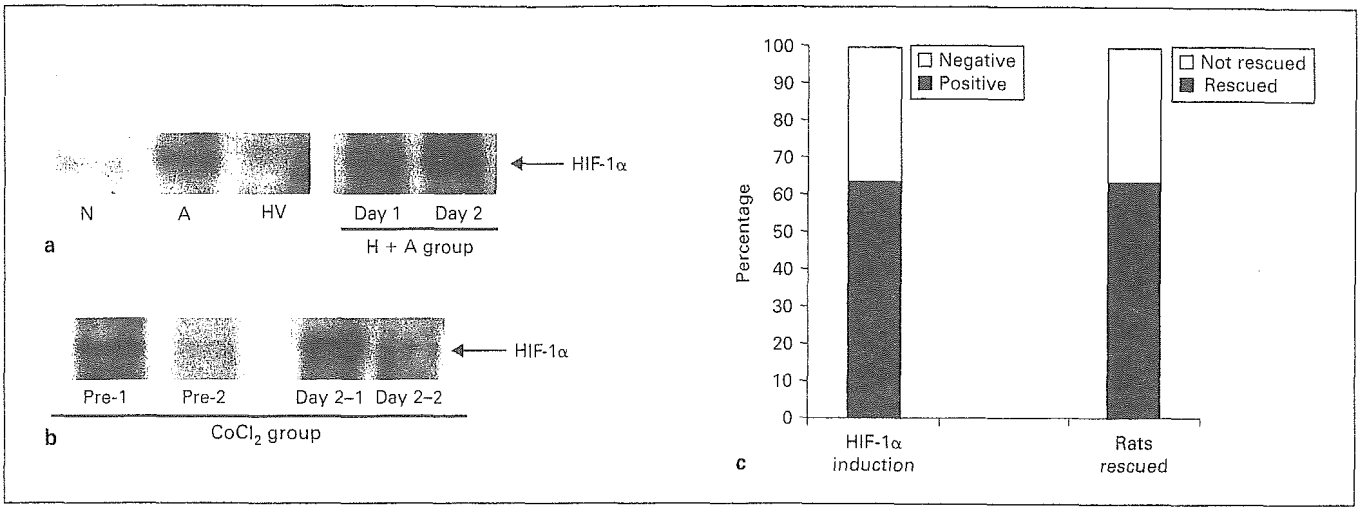

5

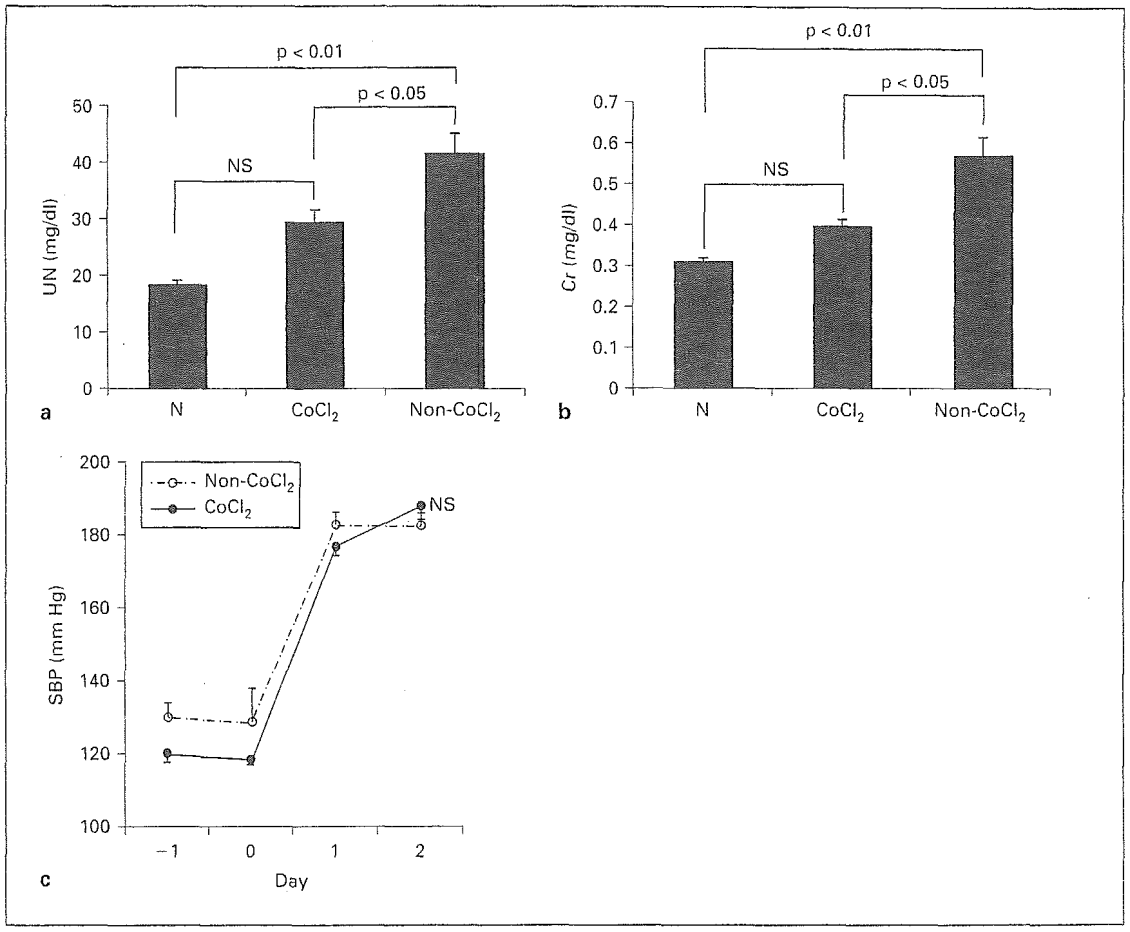

6

Fig. 5. The protein level of HIF-1α is increased by administration of HV and AII, and pretreatment of $CoCl_2$ increases HIF-1α expression before development of GN. HIF-1α is not detected in the N and HV groups (Day 2). However, HIF-1α is detected in A (Day 2) and H+A (Days 1 and 2) groups (**a**). The $CoCl_2$ group, in accord with the level of HIF-1α induction, was divided into 2 groups. HIF-1α is greatly induced before the development of GN ($CoCl_2$ group Pre-1), and is followed by a high level ($CoCl_2$ group Day 2-1); in contrast, it is not efficiently induced ($CoCl_2$ group Pre-2), and also is scarcely detected on day 2 ($CoCl_2$ group Day 2-2) (**b**). The rate of preinduction of HIF-1α by $CoCl_2$ is comparable with that of the inhibition of GN by $CoCl_2$ (**c**).

Fig. 6. Pretreatment with $CoCl_2$ attenuates GN. Serum UN (**a**) and Cr (**b**) levels in the $CoCl_2$ group on day 2 are significantly decreased compared to those in the non-$CoCl_2$ group. There is no significant difference in SBP between the $CoCl_2$ and non-$CoCl_2$ groups (**c**).

HV and AII. Many models of GN have been reported including 5/6 nephrectomized and Thy-1.1 nephritis models [18, 19]. However, these models take a long time to develop nephropathy. In contrast, our protocol induced GN in 2 days, suggesting that one of the advantages our model has over others is in terms of the time course. Further, pathological findings were restricted to glomerular regions without remarkable tubular or interstitial lesions. Since our GN model developed within 2 days, it also has advantages for disclosing the specifically critical time point of the development of GN. Furthermore, the development rate of GN was almost 100%, indicating the high reproducibility of our model. This basis of the rat model was initially developed by Barnes et al. [20] who reported that the progression of AII-induced renal injury was accelerated by pre-existing injury induced by HV; our model, which now optimizes the reproducibility of GN, is a modification of theirs.

Habu-induced nephropathy was reported to develop within 1 day by a dose of 2.0–4.0 mg/kg HV (in our model 3.5 mg/kg) and the main pathological change was 'mesangiolysis' [21, 22]. However, for reasons we have not as yet ascertained, in our study no rats showed Habu-nephropathy-specific pathological findings during the first week in the HV group. On the other hand, AII is one of the major factors responsible for the pathogenesis of GN, because it remarkably increases glomerular pressure causing hyperfiltration, production of extracellular matrix and expression of lines of genes involving GN [23–25]. Further, since AII has some ischemic effects on the kidneys, there is the possibility that an AII-induced ischemic effect causes the GN depicted in our model. However, as demonstrated in this study, glomerular injury was predominantly observed, and was not associated with renal tubular lesions, i.e. tubular necrosis suggesting renal ischemia. Therefore, in accordance with the pathological characteristic of this GN, AII-induced renal ischemia may not be responsible for its development in our model. Additionally, in this study, SBP increased in the A and H+A groups, but GN was not induced in the A group. Therefore, GN in our model was induced not by HV or AII alone, but by the combination of HV and AII, independent of any increase in systemic blood pressure.

HIF-1α is a master transcriptional factor, transactivating the expression of many genes important for cell survival under hypoxic conditions [11–13, 26]. These genes are responsible for glycolysis, angiogenesis, proliferation and iron metabolism, all of which are induced by hypoxic stress; thus, the induction of HIF-1α is a marker of hypoxia. HIF-1α is regulated at the post-translational level by the proteasome system through ubiquitination with von Hippel-Lindau (VHL) protein [27, 28]. As previously reported, this regulation of HIF-1α protein level is dependent on the concentration of oxygen. Hypoxia induces enhancement of HIF-1α protein stability leading to the elevation of the protein level due to inhibition of degradation by VHL. Therefore, hypoxia induces adaptation in cells including induction of HIF-1α; the hypoxic pathway. On the other hand, a line of evidence recently accumulated suggests that HIF-1α is also regulated independently of oxygen concentration through the nonhypoxic pathway [14, 15]. AII is reported to regulate HIF-1α both at transcriptional and post-translational levels in vascular smooth muscle cells cultured under normoxic condition through the AII type 1 receptor [14, 15]. Moreover, HIF-1α is also post-translationally regulated in several cell lines in the presence of tumor necrosis factor-α or nitric oxide independent of oxygen contents [29, 30].

As demonstrated in this study, immunoreactivity of HIF-1α was not detected in the N group (no treatment group), but HIF-1α was detected in the nuclei of glomerular, tubular and epithelial cells of the papilla by administration of AII alone or AII and HV together. This is the first evidence showing that HIF-1α was detected in the kidney by AII, independent of systemic hypoxic stress. As indicated here, HIF-1α was found to be expressed only in intact, not damaged glomeruli. Even within a glomerulus, only the intact part of glomerular cells expressed HIF-1α. Considering the fact that induction of HIF-1α is one of the defense mechanisms for cell survival [31–33], our data indicate that induction of HIF-1α is a marker of glomeruli survival; indeed, it could be a marker of renal protection.

To further investigate whether HIF-1α is involved in the progression or protection of GN, preinduction of HIF-1α was performed with $CoCl_2$ before administration of HV and AII. Surprisingly, the induction of HIF-1α by $CoCl_2$ pretreatment attenuated the progression of GN; the level of GN was reduced from 44.9 to 12.2% and the incidence of GN was reduced from 100 to 36.4%. Furthermore, as indicated, the preinduction of HIF-1α actually affects the inhibition of GN, because the rate of HIF-1α induction was parallel with that of the attenuation of GN. Therefore, our data suggest that HIF-1α is involved, at least in part, in the defense mechanism against the progression of GN, and hence could be a marker for renal protection.

AII is reported to induce HIF-1α [14, 15] and plays a partial role in the renal protective effect; however, the other effects of AII, such as increasing glomerular pressure and modulating gene expression involving in the renal

failure, may overcome any protective effect of AII-induced HIF-1α, and so as a result it may lead to the progression of GN.

In conclusion, we developed a highly reproducible GN model by combining HV and AII. Preinduction of HIF-1α remarkably attenuated the progression of GN, indicating that HIF-1α was involved in the defense mechanism of the kidney.

Acknowledgments

This work was supported by Grants-in-Aid for Scientific Research from the Ministry of Education, Science and Culture (No. 14657409). We thank Dr. Masami Nakatani, Dr. Noriko Kishimoto, Dr. Ichiro Yamasaki, Dr. Yoshitaka Kumon, Dr. Hiroaki Takeuchi, Dr. Jun Imamura, Dr. Mikio Kamioka, Ms. Chiaki Kawada, Ms. Chizuko Sugimoto, and Mr. Takuya Yamaguchi for their helpful advice and generous support.

References

1 Rifai A, Small PA Jr, Teague PO, Ayoub EM: Experimental IgA nephropathy. J Exp Med 1979;150:1161–1173.
2 Ishizaki M, Masuda Y, Fukuda Y, Yamanaka N, Masugi Y, Shichinohe K, Nakama K: Renal lesions in a strain of spontaneously diabetic WBN/Kob rats. Acta Diabetol Lat 1987;24:27–35.
3 Banks KL: Glomerulonephritis, autoimmunity, autoantibody. Animal model: Anti-glomerular basement membrane antibody in horses. Am J Pathol 1979;94:443–446.
4 Elzinga LW, Rosen S, Bennett WM: Dissociation of glomerular filtration rate from tubulointerstitial fibrosis in experimental chronic cyclosporine nephropathy: Role of sodium intake. J Am Soc Nephrol 1993;4:214–221.
5 Arendshorst WJ, Finn WF, Gottschalk CW: Pathogenesis of acute renal failure following temporary renal ischemia in the rat. Circ Res 1975;37:558–568.
6 Wilson CB, Dixon FJ: Immunopathologic mechanisms of renal disease. Ric Clin Lab 1975;5:17–38.
7 Masuda Y, Shimizu A, Mori T, Ishiwata T, Kitamura H, Ohashi R, Ishizaki M, Asano G, Sugisaki Y, Yamanaka N: Vascular endothelial growth factor enhances glomerular capillary repair and accelerates resolution of experimentally induced glomerulonephritis. Am J Pathol 2001;159:599–608.
8 Kim S, Iwao H: Molecular and cellular mechanisms of angiotensin II-mediated cardiovascular and renal diseases. Pharmacol Rev 2000;52:11–34.
9 Lee LK, Meyer TW, Pollock AS, Lovett DH: Endothelial cell injury initiates glomerular sclerosis in the rat remnant kidney. J Clin Invest 1995;96:953–964.
10 Huang LE, Arany Z, Livingston DM, Bunn HF: Activation of hypoxia-inducible transcription factor depends primarily upon redox-sensitive stabilization of its alpha subunit. J Biol Chem 1996;271:32253–32259.
11 Wang, GL, Jiang BH, Rue EA, Semenza GL: Hypoxia-inducible factor 1 is a basic-helix-loop-helix-PAS heterodimer regulated by cellular O_2 tension. Proc Natl Acad Sci USA 1995;92:5510–5514.
12 Rosenberger C, Mandriota S, Jurgensen JS, Wiesener MS, Horstrup JH, Frei U, Ratcliffe PJ, Maxwell PH, Bachmann S, Eckardt KU: Expression of hypoxia-inducible factor-1alpha and -2alpha in hypoxic and ischemic rat kidneys. J Am Soc Nephrol 2002;13:1721–1732.
13 Wenger RH, Rolfs A, Marti HH, Guenet JL, Gassmann M: Nucleotide sequence, chromosomal assignment and mRNA expression of mouse hypoxia-inducible factor-1 alpha. Biochem Biophys Res Commun 1996;223:54–59.
14 Richard DE, Berra E, Pouyssegur J: Nonhypoxic pathway mediates the induction of hypoxia-inducible factor 1alpha in vascular smooth muscle cells. J Biol Chem 2000;275:26765–26771.
15 Page EL, Robitaille GA, Pouyssegur J, Richard DE: Induction of hypoxia-inducible factor-1alpha by transcriptional and translational mechanisms. J Biol Chem 2002;277:48403–48409.
16 Raij L, Azar S, Keane W: Mesangial immune injury, hypertension, and progressive glomerular damage in Dahl rats. Kidney Int 1984;26:137–143.
17 Linas SL, Shanley PF, Whittenburg D, Berger E, Repine JE: Neutrophils accentuate ischemia-reperfusion injury in isolated perfused rat kidneys. Am J Physiol 1988;255:F728–F735.
18 Romero F, Rodriguez-Iturbe B, Parra G, Gonzalez L, Herrera-Acosta J, Tapia E: Mycophenolate mofetil prevents the progressive renal failure induced by 5/6 renal ablation in rats. Kidney Int 1999;55:945–955.
19 Kaneko Y, Shiozawa S, Hora K, Nakazawa K: Glomerulosclerosis develops in Thy-1 nephritis under persistent accumulation of macrophages. Pathol Int 2003;53:507–517.
20 Barnes JL, Lisa MS: Origin of interstitial fibroblasts in an accelerated model of angiotensin II (AII)-induced interstitial fibrosis. J Am Soc Nephrol 2001;12:699A3645.
21 Cattell V, Bradfield JW: Focal mesangial proliferative glomerulonephritis in the rat caused by habu snake venom. A morphologic study. Am J Pathol 1977;87:511–524.
22 Kitamura H, Sugisaki Y, Yamanaka N: Endothelial regeneration during the repair process following Habu-snake venom induced glomerular injury. Virchows Arch 1995;427:195–204.
23 Ruggenenti P: Angiotensin-converting enzyme inhibition and angiotensin II antagonism in nondiabetic chronic nephropathies. Semin Nephrol 2004;24:158–167.
24 Tolins JP, Raij L: Effects of amino acid infusion on renal hemodynamics. Role of endothelium-derived relaxing factor. Hypertension 1991;17:1045–1051.
25 Nakamura T, Obata J, Kimura H, Ohno S, Yoshida Y, Kawachi H, Shimizu F: Blocking angiotensin II ameliorates proteinuria and glomerular lesions in progressive mesangioproliferative glomerulonephritis. Kidney Int 1999;55:877–889.
26 Makino Y, Cao R, Svensson K, Bertilsson G, Asman M, Tanaka H, Cao Y, Berkenstam A, Poellinger L: Inhibitory PAS domain protein is a negative regulator of hypoxia-inducible gene expression. Nature 2001;414:550–554.
27 Neckers LM: aHIF: The missing link between HIF-1 and VHL? J Natl Cancer Inst 1999;91:106–107.
28 Maxwell PH, Wiesener MS, Chang GW, Clifford SC, Vaux EC, Cockman ME, Wykoff CC, Pugh CW, Maher ER, Ratcliffe PJ: The tumour suppressor protein VHL targets hypoxia-inducible factors for oxygen-dependent proteolysis. Nature 1999;399:271–275.
29 Zhou J, Fandrey J, Schumann J, Tiegs G, Brune B: NO and TNF-alpha released from activated macrophages stabilize HIF-1alpha in resting tubular LLC-PK1 cells. Am J Physiol Cell Physiol 2003;284:C439–C446.
30 Sandau KB, Zhou J, Kietzmann T, Brune B: Regulation of the hypoxia-inducible factor 1alpha by the inflammatory mediators nitric oxide and tumor necrosis factor-alpha in contrast to desferroxamine and phenylarsine oxide. J Biol Chem 2001;276:39805–39811.
31 Prass K, Ruscher K, Karsch M, Isaev N, Megow D, Priller J, Scharff A, Dirnagl U, Meisel A: Desferrioxamine induces delayed tolerance against cerebral ischemia in vivo and in vitro. J Cereb Blood Flow Metab 2002;22:520–525.
32 Furuta GT, Turner JR, Taylor CT, Hershberg RM, Comerford K, Narravula S, Podolsky DK, Colgan SP: Hypoxia-inducible factor 1-dependent induction of intestinal trefoil factor protects barrier function during hypoxia. J Exp Med 2001;193:1027–1034.
33 Matsumoto M, Makino Y, Tanaka T, Tanaka H, Ishizaka N, Noiri E, Fujita T, Nangaku M: Induction of renoprotective gene expression by cobalt ameliorates ischemic injury of the kidney in rats. J Am Soc Nephrol 2003;14:1825–1832.

循環器科，58(6)：600-605，2005

特集 先駆的医工学と循環器

バイオニック動脈圧反射による血圧コントロール*

佐藤隆幸**

Key Words : arterial pressure, baroreflex failure, bionics, orthostatic hypotension, sympathetic nerve

はじめに

最近の老年医学研究により，加齢に伴う動脈圧反射障害が起立性低血圧をひき起こし，廃用症候群(いわゆる寝たきり)の重要な誘因であることが明らかになりつつある．また，中高年を好発年齢とする進行性の神経変性疾患，たとえば，シャイ・ドレーガー症候群・多系統萎縮症，あるいは，外傷による高位脊髄損傷などでは，生命維持にきわめて重要な血管運動中枢が侵されたり，交感神経遠心路障害により圧反射機能が廃絶するため，重度の起立性低血圧や起立性失神を起こすようになる．多くの場合，最終的には寝たきり状態となる[1)~3)]．

このように起立性低血圧は，生活の質を著しく低下させる重要な病態であるが，多くの場合，根治的治療法はない．これまでに，薬物療法と心臓ペースメーカによる頻拍ペーシングが試されてきたがいずれも無効であった[4)5)]．血管収縮剤やミネラルコルチコイドによる薬物療法の場合，仮に，起立時の低血圧を防止することに成功しても，臥位時の重症高血圧をまねくことがあった．また，頻拍ペーシングは動脈圧調節の前負荷(中心静脈圧)依存性を増強し，むしろ起立性低血圧を悪化させることがあった．このようなことから，ヒトの体位変換時の血圧調節に絶対的に重要な圧反射機能を再建することこそが治療の唯一の方法であると認識されるようになってきた．

そこで著者らは，圧反射機能を再建する医工学的アプローチとしてバイオニック圧反射装置を開発し，その有効性を術中の起立性低血圧モデルで検証し，臨床応用への道を模索している[6)~8)]．

バイオニック動脈圧反射装置の開発

1．開発の原理

動脈圧反射は，さまざまな外乱による脳の灌流圧変化を抑制する機構としてはたらくきわめて重要なフィードバック制御システムである[9)~11)]．時々刻々と変化する動脈圧は，頸動脈洞や大動脈弓の圧受容器で検知され，圧受容器神経活動として血管運動中枢にフィードバックされる．血管運動中枢はこの圧受容器神経活動に応じて，交感神経活動を変化させる．その結果，血管の収縮・弛緩が生じ，外乱の影響が抑制されることになる．したがって，動脈圧反射は，重力環境下での臥位から立位への体位変換時の血圧低下，すなわち起立性低血圧を防止する血圧制御機構として必須である．動脈圧反射失調では，

* Bionic baroreflex control of arterial pressure.

** Takayuki SATO, M.D., Ph.D.: 高知大学医学部循環制御学教室〔〒783-8505 南国市岡豊町小蓮〕; Department of Cardiovascular Control, Kochi Medical School, Nankoku 783-8505, JAPAN

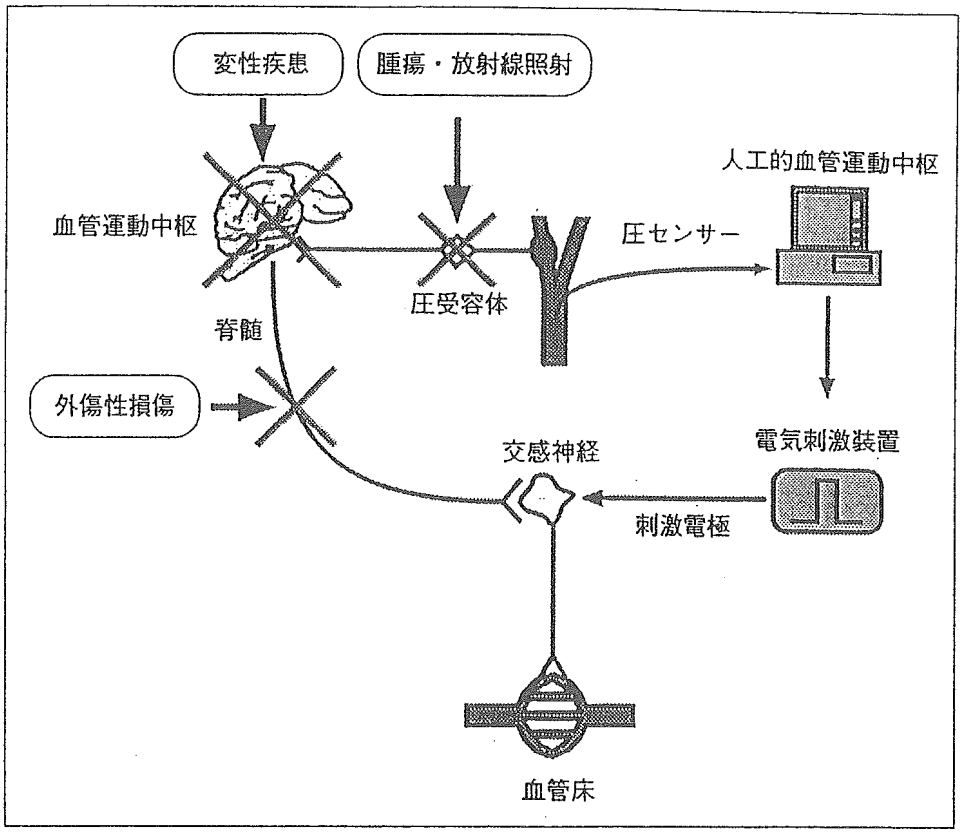

図1　動脈圧反射障害をきたす病態とバイオニック動脈圧反射装置

これら一連の反射性血圧調節が作動しないため，起立性低血圧が必発となる．したがって，このような患者を救うためには，機能廃絶した血管運動中枢の機能代行装置として，人工的血管運動中枢を有した血圧制御装置が必要となる．

バイオニック動脈圧反射装置の動作原理は，図1のように，「血圧を常時監視しながら，実時間演算で交感神経の電気刺激頻度を決定する」というものである．すなわち，本装置は，圧センサー→人工的血管運動中枢(コンピュータ)→電気刺激装置→交感神経→血管床からなるフィードバック血圧制御装置である[6)~8)]．

2．理論的背景[12)]

バイオニック動脈圧反射における情報の流れをブロック線図にすると図2のようになる．制御工学の分野で古典的に用いられる積分・比例補償型のフィードバック制御の理論を応用した．現在の血圧値の設定値からのずれにもとづいて交感神経の刺激頻度を決定する人工的血管運動中枢，すなわち制御部の伝達関数を$H_1(f)$とする．伝達関数は周波数領域での入出力関係を記述したものである．また，交感神経の刺激頻度の変化に対する血圧応答に関する効果器の伝達関数を$H_2(f)$とする．

現在の血圧値$AP(f)$の設定値$AP_t(f)$からのずれ$E(f)$は，

$$E(f)=AP_t(f)-AP(f) \quad \cdots\cdots (1)$$

と表される．$H_1(f)$は，比例補償係数K_pと積分補償係数K_iおよびラプラス演算子$s=2\pi fj$を用いると次のように表される．

$$H_1(f)=K_p+\frac{K_i}{s} \quad \cdots\cdots (2)$$

また，

$$STM(f)=E(f)\cdot H_1(f) \quad \cdots\cdots (3)$$

となる．

一方，現在の血圧値は，交感神経の刺激頻度の変化と外乱$AP_d(f)$によって変動することから，

$$AP(f)=STM(f)\cdot H_2(f)+AP_d(f) \quad \cdots (4)$$

最終的に，外乱の影響が現在の血圧値にどのように反映されるかは，式(1)，(3)，(4)を整頓して，

$$AP(f)=\frac{H_1(f)H_2(f)}{1+H_1(f)H_2(f)}AP_t(f)+\frac{1}{1+H_1(f)H_2(f)}AP_d(f)$$

となることから明らかなように，バイオニック

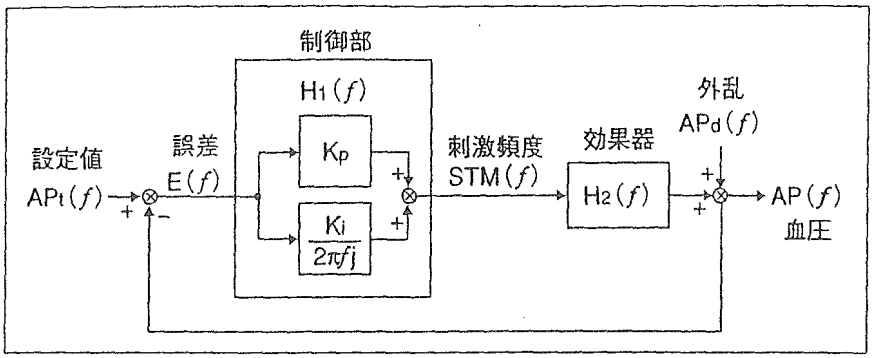

図2　バイオニック動脈圧反射におけるブロック線図
生体本来の動脈圧反射と同様に，バイオニック動脈圧反射では，血圧を乱そうとする外乱の影響を抑制して血圧の安定化をはかる．

動脈圧反射装置を用いたフィードバック制御により，$1/[1+H_1(f)H_2(f)]$に抑制されることがわかる．

以上のようなことから，バイオニック動脈圧反射装置が有効に働くようにするためには，式(2)におけるK_pとK_iが適切に決定されることが必要になる．具体的には，人工的血管運動中枢として働くコンピュータのプログラムが有効性の鍵を握っているということになる．

われわれは，$H_2(f)$を実験的臨床研究によって求め，K_pとK_iについては，数値シミュレーションによってもっとも有効に外乱の影響を抑えることが可能な値に決定し，$H_1(f)$を最適化した．

3．ヒトの交感神経刺激法と刺激に対する血圧の応答特性

これまでの動物実験や臨床研究から，胸腰髄レベルに留置した硬膜外カテーテル電極により，効率よく動脈圧を制御可能であることが判明している[6~)8)13)~15)]．そこで，変形性頸椎症・頸椎椎間板ヘルニア・後縦靱帯骨化症などの手術時に術中脊髄機能モニタリングとして，脊髄誘発電位記録を行う患者を対象として，不規則に電気刺激を行いながら血圧応答を記録した．12例の患者からデータを取得し，$H_2(f)$を推定した．脊髄の刺激に応じて血圧が変動していることがわかる．

脊髄刺激頻度の変化を入力，血圧応答を出力として推定された伝達関数の結果を図3-Bに示す．平均的な伝達関数$H_2(f)$を求めるために，下記の二次の低域通過フィルターへの曲線近似法を用いて解析した．

$$H_2(f)=\frac{a}{1+2\zeta\left(\frac{f}{f_N}j\right)+\left(\frac{f}{f_N}j\right)^2}\exp(-2\pi f jL)$$

なお，aは定常ゲイン，ζは減衰係数，f_Nは固有周波数，Lはラグ時間である．その結果，それぞれ，0.4, 2.6, 0.06Hz, 9秒という結果が得られた．

4．人工的血管運動中枢の設計

近似$H_2(f)$を用いて，ステップ状の血圧低下(−20mmHg)に対するバイオニック動脈圧反射の振る舞いを比例補償係数$K_p=0, 1, 2$，積分補償係数$K_i=0, 0.01, 0.05, 0.1, 0.2$の組合わせでシミュレーションした．$K_p$と$K_i$の両者が0の場合には，外乱の影響はまったく圧縮されない(図4-A～Cの実線)．

$K_p=0$の場合，全体的に血圧応答が緩徐である．K_iの増加に従い，立上がり時間(rise time, T_r)および整定時間(settling time, T_s)の短縮がみられるが，K_iが0.05を超えると不足減衰応答(under-damped response)がみられるようになり，動脈圧反射が不安定になってくる．

$K_p=2$の場合，T_rは短く応答は迅速であるが，K_iの値にかかわらず動脈圧反射は不安定である．

$K_p=1$の場合，動脈圧反射は，$K_p=0$に比べ迅速で，K_iが0.1になるまでほとんど振動はみられない．$K_i=0.1$のとき，T_rは約50秒で，T_sは60秒以内であった．動脈圧反射の迅速な応答と安定性の両者を満たすものとして，この付近の条件が適していると考えられた．

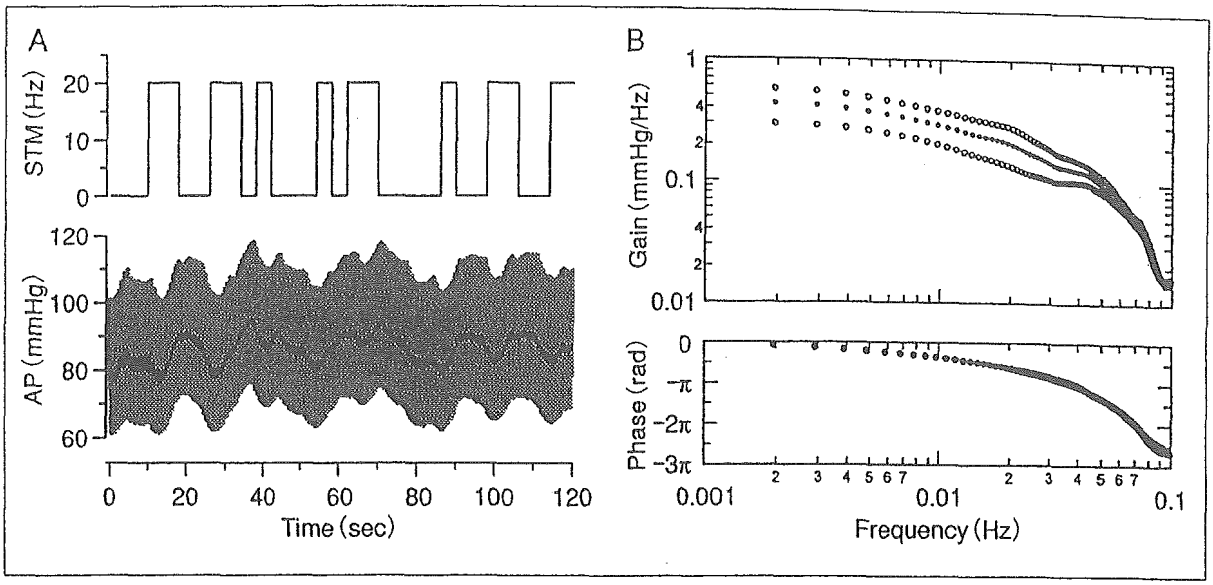

図3

A：不規則な脊髄交感神経刺激に対する血圧応答．刺激頻度(STM)を0か20ヘルツに不規則に変化させ，血圧応答(AP)を記録した．B：刺激頻度の変化に対する血圧応答の動的な特性を示す伝達関数．黒丸が平均値で白丸が平均±標準偏差(12例)を示す．

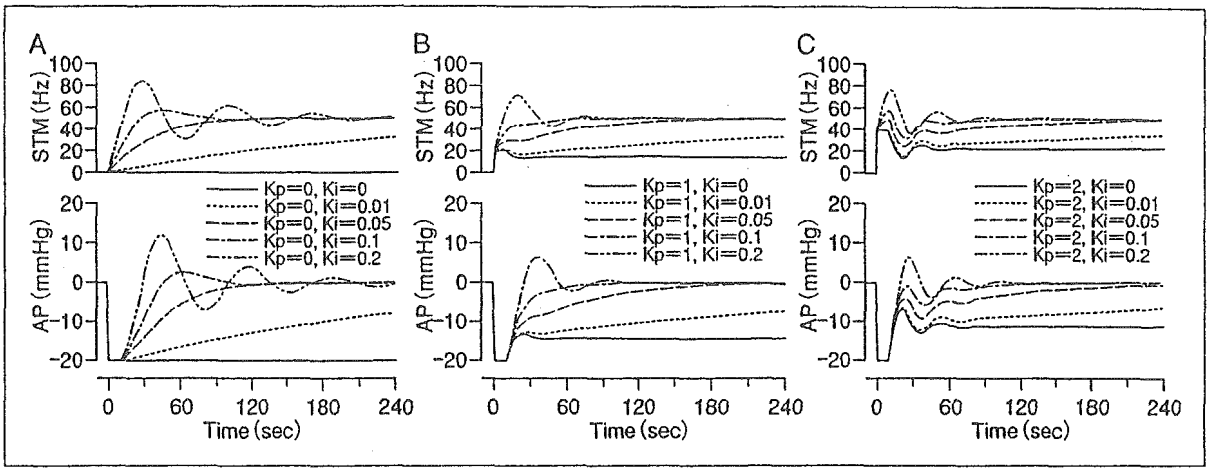

図4　人工的血管運動中枢の設計のためのシミュレーション

図2における比例補償係数(K_p)と積分補償係数(K_i)の組合わせを変えて，−20mmHgの外乱の影響がどのように表れるかを数値解析した．補償係数がともにゼロの場合には，外乱の影響はまったく抑制されない．

バイオニック動脈圧反射装置の有効性の検証

上記の結果を用いて，人工的血管運動中枢を設計し，試作したバイオニック動脈圧反射装置の有効性を検証した．検証にあたっては，起立性低血圧と同様，あるいは類似の血行動態変化による急激でかつ再現性のある低血圧モデルが理想的である．そこで，下肢人工関節置換術の際に止血目的で大腿部に圧迫帯を用いる症例に着目した．このような症例では，圧迫帯の解除時に急激な低血圧を生ずることが知られている[16)17)]．バイオニック動脈圧反射装置の作動中に圧迫解除を行った場合と，そうでない場合で，血圧がどのように変化するかを検討した．22例から得られた結果は，図5に示されている．大腿部の圧迫止血帯の急速解除に伴う血行動態は，解除後急激に血圧と中心静脈圧が低下した．これは，圧迫解除に伴う下肢への血液貯留により静脈還流が減少し心拍出量が減少したことと，大腿動脈の圧迫解除によって血管床の相対的増加がもたらされ，血管抵抗が減少したことを示